We are IntechOpen, the world's leading publisher of Open Access books
Built by scientists, for scientists

4,800
Open access books available

122,000
International authors and editors

135M
Downloads

154
Countries delivered to

Our authors are among the

TOP 1%
most cited scientists

12.2%
Contributors from top 500 universities

CLARIVATE ANALYTICS
BOOK CITATION INDEX
INDEXED

WEB OF SCIENCE™

Selection of our books indexed in the Book Citation Index
in Web of Science™ Core Collection (BKCI)

Interested in publishing with us?
Contact book.department@intechopen.com

CO₂ Utilization: A Process Systems Engineering Vision

Ofélia de Queiroz F. Araújo,
José Luiz de Medeiros and Rita Maria B. Alves

Additional information is available at the end of the chapter

1. Introduction

The development of economies results in increased energy consumptions, as observed in Figure 1. In the coming decades, the supply of such expanding demand will remain based on fossil fuels technologies. Expanding the share of renewable energy (*e.g.*, biofuels in the case of transportation fuels) would require massive investments in creating a new infrastructure, which would eventually raise the standards to a new economic order entirely based on renewables in the near future. On the other hand, the current scenario involves the announcement of large proven reserves of non-conventional gas and oil and expansion of installed infrastructure of production and refining.
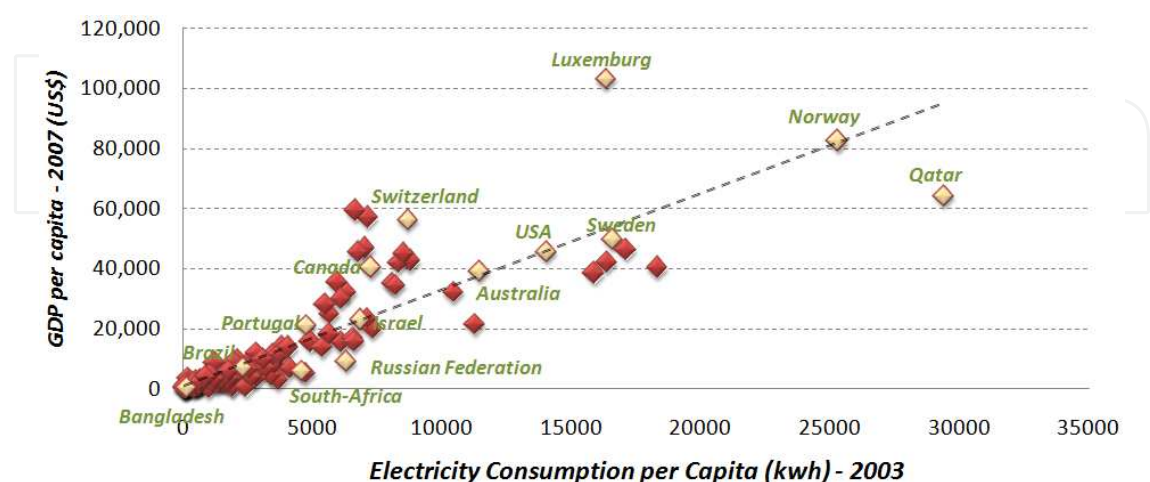

Figure 1. Economic development and electricity consumption. [graph constructed with data available at hdr.undp.org]

Fossil fuel based energy is recognized as carbon emitter. The challenge of the century is thus to expand energy supply in a carbon-constrained economy. According to the World Economic Forum (King, 2010), no truly low-carbon technology will be able to penetrate the mass market in the short term. The use of installed fossil processing infrastructure, with co-processing of biomass and fossil feedstock and capturing and utilization of emitted CO_2 is the "escape route" for a moderate transition from the present to a long-term sustainable future. In this context, putting a price on carbon will gradually build the road to a greener tomorrow. Meanwhile, bio-based products are a realistic supplement to fossil-based products, but they cannot mitigate the rising demand for fossil fuels.

According to an IEA Technology Roadmap, the manufacture of only 18 chemicals account for 80% of the energy demand in the chemical industry and 75% of its greenhouse gas (GHG) emissions. The study concludes that, "in the short to medium term (to 2025), steady progress in implementing incremental improvements and deploying best practice technologies (BPT) could provide substantial energy savings and emissions reductions compared to business as usual". "A step change in the sector's energy consumption and GHG emissions would require the development of 'game changer' technologies, such as sustainable biomass feedstocks and hydrogen from renewable energy sources which have not yet reached commercial maturity." (IEA, 2013)

With this prospect, CO_2 utilization in the short term should allow parallel production routes based on BPT, driven by emission-capture-utilization synergies. In this sense, production and conversion of synthesis gas (SYNGAS) exhibits the highest potential for medium term of commercial success. Nevertheless, it is worth noting that, while the utilization of CO_2 has potential to reduce greenhouse gas emissions into the atmosphere, CO_2 has disadvantages as a chemical reactant due to its relative significant chemical inertness. This inertness is the underlying reason why CO_2 has broad industrial application as solvent (supercritical CO_2), as fire and pest extinguisher, and as a non-toxic amusement additive in the food industry. From the standpoint of building a low-carbon economy, each potential use of CO_2 as reactant has a customarily high energy requirement, entailing associated energy-related GHG emissions. Obviously, such GHG emissions should not exceed the yield of chemical conversion of CO_2. Reverse water gas shift (RWGS) and dry reforming to yield SYNGAS and CO_2 hydrogenation to methanol are the most prominent CO_2 conversion alternatives to high volume chemical commodities. On the other hand, it is reasonable to expect that CO_2 conversion and biomass-based processing alternatives will coexist for a while with fossil-based technologies. Figure 2 illustrates the concept of co-existing fossil and biomass feedstock, having SYNGAS generation as the integration phase. In this scenario, SYNGAS can be obtained from coexisting fossil and green feedstock via gasification (of biomass, coal and heavy residues), steam reform and dry (CO_2) reform of natural gas, which, in turn, will also coexist with downstream nonconventional conversion routes – e.g., Fischer-Tropsch (FT) and methanol to olefins (MTO) – to fuels and chemical intermediates to supply the installed petrochemical industries.

In countries with large bioresources as well as significant oil and natural gas production infrastructure (e.g., USA, Canada, Mexico, China, Russia, Australia, Argentina and Brazil), fossil feedstock (mainly nonconventional oil and gas) will present the greatest challenge to bio-

mass. In Brazil, for instance, gas supply capacity in Santos Basin increased from 600 thousand m^3/d, in 2009, to 22.2 million m^3/d in 2013 (PETROBRAS, 2013). The identified risks associated to such expansion are, beside depletion of natural resources, increased CO$_2$ emissions.

Therefore, CO$_2$ capture, transportation and utilization must be included in the scene since CO$_2$ stands conceptually as a renewable feedstock. In this sense, Figure 3 illustrates CO$_2$ emissions capture and utilization associated to the production and refining of fossil fuel. It is worth noting that, in addition to the variety of alternative technologies, other factors influence the conception of capture and utilization of CO$_2$ for the production of chemicals.

Rostrup-Nielsen and Christiansen (2011) present four recognizable trends in next generation successful plants for producing chemical commodities: (a) location of cheap raw materials; (b) economy of scale; (c) highly integrated process plants; and (d) low CO$_2$ footprint (t CO$_2$/t product) Consequently, the production chain and the associated GHG emissions are complex and require a system view for optimal decision making on technologies for production of energy and chemicals taking into account the CO$_2$ perspective.
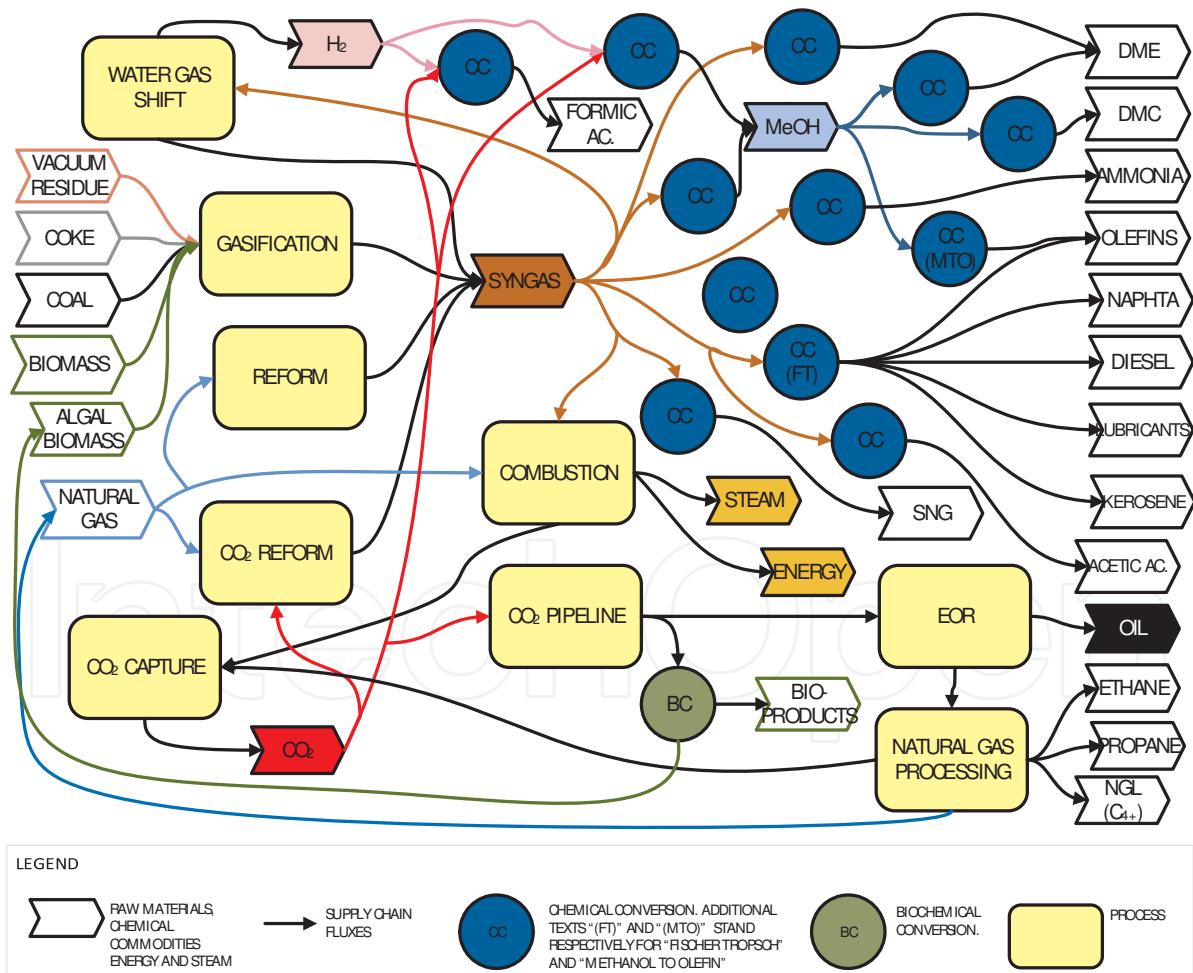

Figure 2. Coexistence of fossil and biomass feedstock uses: CO$_2$ capture and utilization dropped into existing production infrastructure

Chemical Process Systems Engineering (cPSE) deals with the set of basic unit operations involved in turning raw materials into products via chemical and bio-chemical processes. In a wider definition, PSE is concerned with the optimization of decision-making process for creation and operation of chemical supply chains. Such integrated framework embraces product and process design, manufacture and distribution of chemical products with multiple and conflicting technical, economic, energetic, environmental and social objectives.

With this vision, c-PSE of industrial use and reuse of CO_2 supply chain is assessed in a life cycle approach of technological alternatives involving integration of CO_2 capture (separation), CO_2 transportation and CO_2 chemical/biochemical utilization. Apart the conventional utilizations of CO_2 listed above, there are three new potential chains of CO_2 utilizations, namely: (i) production of chemicals via chemical conversion (CC); (ii) enhanced oil recovery (EOR) and carbon geological storage (CGS); and (iii) conversion via algae and microalgae to biomass or biochemical conversion (BC).
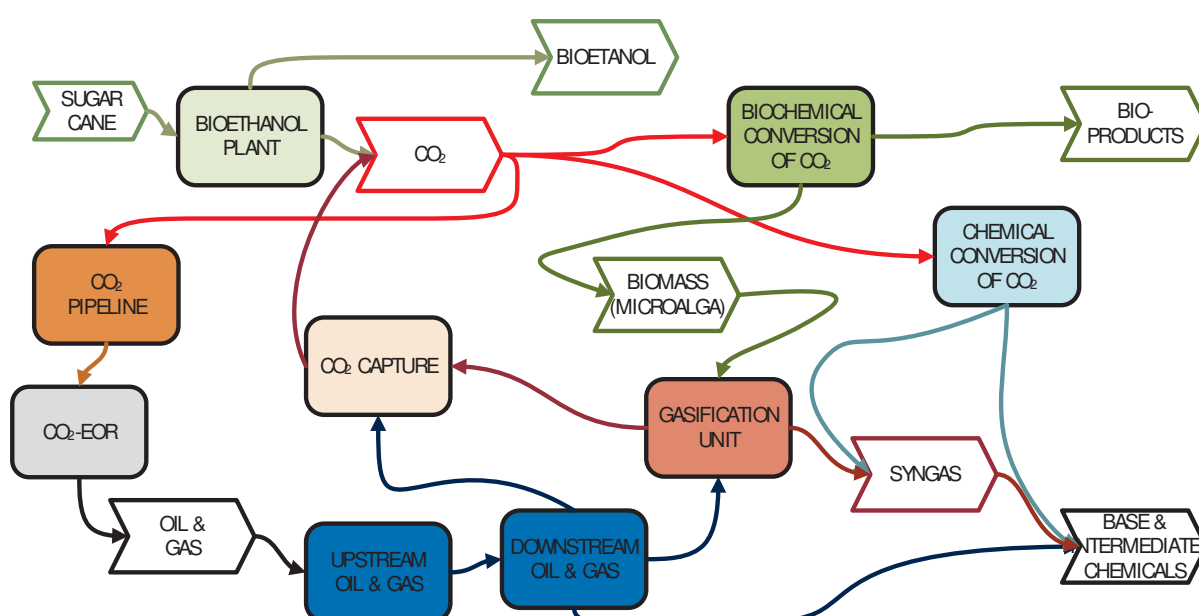

Figure 3. CO_2 capture and utilization in the oil & gas supply chain

EOR and CGS constitute, under present conditions, the only CO_2 processing chain that has some steps ready to be put into operation at high scales. These encompass some separation technologies for CO_2 post-combustion capture, CO_2 compression and CO_2 transportation via long pipelines. EOR and CGS can be reinforced if oxy-fuel technologies finally attain industrial maturity, which may occur within the next 5 decades. Pre-combustion technologies are also potential powerful contributors to EOR-CGS systems, which should be fully developed within the next 5 decades. Pre-combustion relies on some separation technologies also present in post-combustion alternatives.

BC via solar photosynthesis is a promising but still incipient package of technologies that have yet to be proven feasible in large scales. The main drawback is the impressive footprint and liquid hold-up of algae cultivation and processing plants, which have to comply with the high

dispersion and periodicity of solar light and small concentration of biomass in growing medium (always below 10g/L). Besides, the use of non-solar light energy is totally out of question due to the photosynthesis efficiency limitations of green life forms (always below 10%, i.e., only a maximum of 10% of the incident light, already with appropriate wavelength, is biochemically usable to bio-convert CO_2).

CC context encompasses novel approaches extending the technology scenario for CO_2 supply chain via chemical conversion to benign, stable compounds for long-term storage or to value-added products like plastics, chemical intermediates and oxygenated octane enhancers like DMC – dimethyl-carbonate (Souza et al., 2013) for reuse.

The cPSE vision of CO_2 treats routes of CC and BC (and BC integrated with CC, i.e., BCC) to useable products and fuels, not as substitute, but rather as a complement to EOR and CGS. The present text is oriented to analyze CO_2 as a profitable feedstock, i.e., its potential use as feedstock to chemicals and fuels within economic applications, besides its relevant use in EOR. CGS is not considered an economic application; instead, it constitutes only a plausible, secure, destination of the excess of carbon, i.e., all CO_2 that has to be discarded because it is not dispatched to any economic use.

Among the routes for CO_2 utilization, BC is a natural choice as photosynthesis yields biomass, allowing the production of bioproducts, biofuels and chemicals through downstream CC processing routes. In fact, biomass gasification is the most flexible technology for dropping into conventional downstream CC routes. This integrated option configures BCC – biochemical and chemical conversion of CO_2.

The beneficial use of alkaline wastes or metallic ions to convert CO_2 via neutralization of alkaline wastes, or reaction of CO_2 with metallic ions to form less soluble carbonates that can be removed from produced water (oil & gas industry) is also a relevant CC application of CO_2. Lastly, this study presents the EOR use of CO_2, i.e., by injection into depleting oil or gas fields to maximize hydrocarbon production.

Finally, analysis of routes that undertake CO_2 reduction must take into account the life cycle of the processes in order to assess whether additional CO_2 production occurs beyond the amount abated from atmospheric emissions. This is precisely the case of CC of CO_2 into fuels and chemicals that always requires high energy input, normally derived from burning fossil fuels, entailing further associated GHG emissions. In this context, new or mature cPSE solutions should comply with the triple objective of sustainability, namely: economically feasible, environmentally benign and socially beneficial, in a supply chain approach. In connection with this, the chapter presents the CO_2 Capture Cycle as well as promising alternatives of its reutilization.

2. The thermodynamics of pure CO_2

The phase behavior of pure CO_2 (Figure 4) exhibits particularities when compared with common light species of natural gas (NG) like CH_4, C_2H_6 and C_3H_8. In general grounds, CO_2

has a fluid phase behavior similar to ethane (C_2H_6) with a very similar Critical Point (CP) temperature. The pronounced distinctive characteristic is its high Triple Point (TP) (Figure 4) temperature comparatively with light hydrocarbons. This means that solid CO_2 (dry ice) can be easily encountered below -56.6°C and above 5.2bar, if the original processing stream is rich enough in CO_2. This freeze-out of solid is not observed with the light hydrocarbon species unless below -182°C, which is about 20°C below the lowest temperature that can be achieved in LNG processing (i.e., the Normal Boiling Point of CH_4). In other words, without CO_2, the coldest NG processing (LNG plant) does not have solid formation. The phase behavior of pure CO_2 (Figure 4) is characterized by two larger (and infinite) continents corresponding to gas and solid states, and a finite intermediate liquid continent extending between the TP and CP temperatures. The three continents are two-dimensional (2D) objects due to the Phase Rule, which stipulates two degrees of freedom for a pure species at one-phase condition. One-dimensional (1D) equilibrium boundaries – SLE, SVE and VLE lines – are positioned between two neighboring continents. Their 1D nature is also a consequence of the phase Rule, which stipulates one degree of freedom for a pure species at a two-phase condition. SLE – solid-liquid (or solid-fluid) equilibrium line – is an endless line extending from the TP to indefinitely high pressures, characterized by the coexistence of solid and liquid CO_2. SVE – solid-vapor equilibrium line – is characterized by coexistence of solid and gas CO_2 ending at the TP and lower bounded by the absolute 0K. VLE – vapor-liquid equilibrium line – is a finite locus between TP and CP where liquid and gas CO_2 coexist. Just above the liquid continent there is a somewhat indefinite supercritical fluid zone (SCF). The SCF is a fusion of gas and liquid behaviors at high pressures above the CP pressure and high temperatures above the CP temperature. The SCF is characterized by high densities and high compressibility.

The contact point for the three continents is the Triple Point TP, an invariant three-phase point (zero degrees of freedom) by the Phase Rule. The VLE locus ends at the Critical Point CP where the differences between liquid and vapor vanish. The CP is also an invariant point with zero degrees of freedom, but, contrary to the TP, the CP is a single phase point satisfying two extra criticality conditions. The phase behavior of CO_2 depicted in Figure 4 can be enriched if density (kg/m^3) is put on the third axis as shown in Figure 5. In Figure 5, densities of gas phase are calculated via the Peng-Robinson (PR) equation of state (EOS), whereas liquid and solid phase densities (saturated or not) are calculated via the correlations presented by Span and Wagner (1996) and Trusler (2011), respectively. In Figure 5, the saturation lines SLE, SVE and VLE are also depicted, where the VLE line is presented with its gas and liquid branches merging at the CP. Figure 5 reveals that CO_2 can be found with densities well above the density of water (1000 kg/m^3), either as a solid or as high pressure dense liquid or SCF fluid.

The PR-EOS is a very simple thermodynamic relationship that can be used to predict gas and liquid properties of pure CO_2 and of CO_2 rich mixtures. The PR-EOS is certainly not the most accurate state relationship to address the fluid properties of CO_2 (Genesis, 2011; see also the EOS presented by Span and Wagner, 1996), but it does represent the best compromise between simplicity of use and accuracy for CO_2 rich systems without water, either in single fluid phase or in two coexisting fluid phases (VLE), at low or high pressures and densities (Li, 2008; Li and Yan, 2009; Genesis, 2011). According to Genesis (2011), the PR-EOS produces errors for
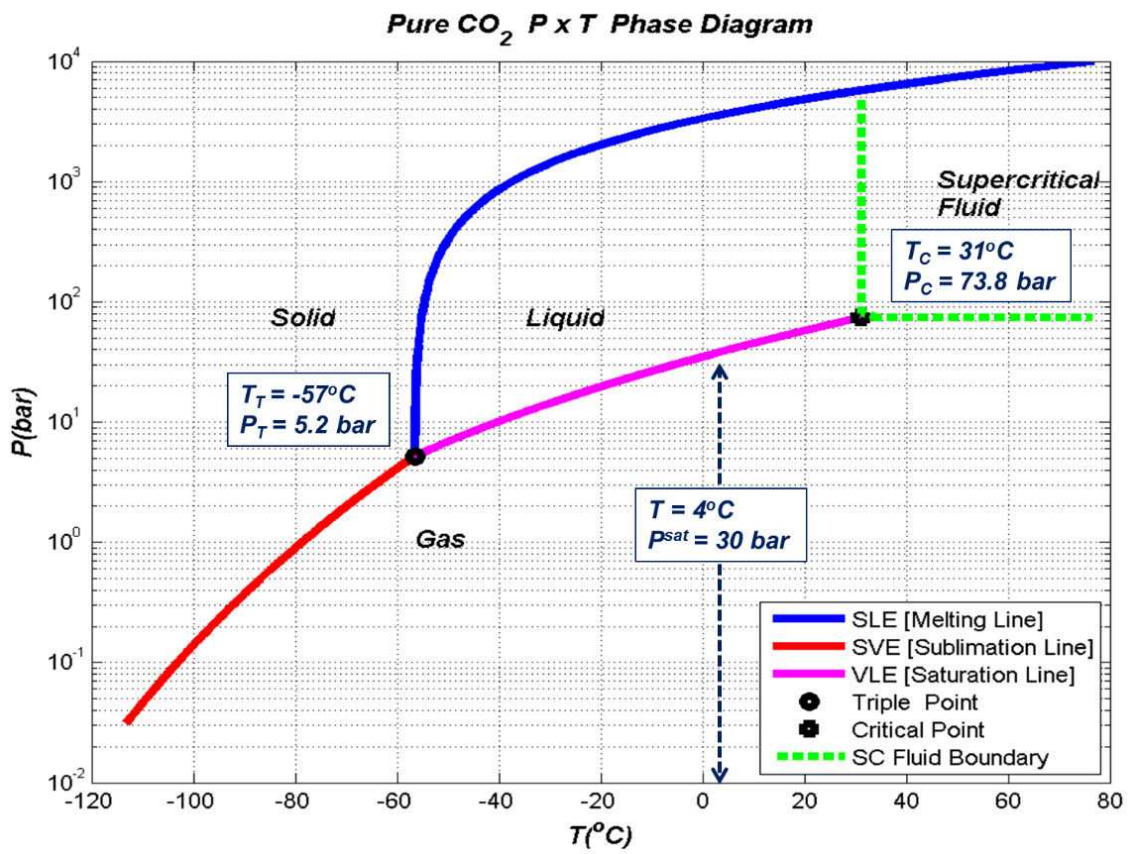
Figure 4. Phase behavior of pure CO$_2$ [T_C, P_C critical point; T_T, P_T triple point]
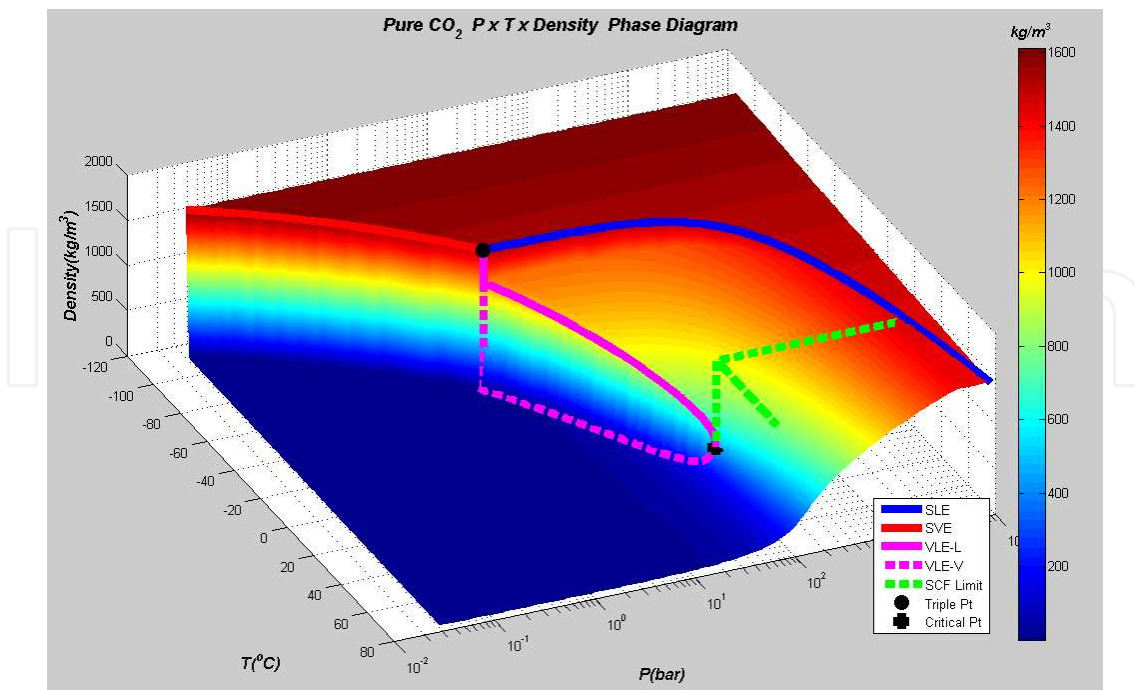

Figure 5. Density x Pressure x Temperature of Pure CO$_2$ [with TP and CP points, VLE, SVE & SLE lines and SCF domain]

compressibility factor (Z), molar enthalpy (H) and sound speed (C) below 1% for CO_2 subcritical gas phases and between 5% and 20% for subcritical liquid phases. Near the CP, the errors in Z, H, C can be higher but the uncertainties of experimental values are also higher. In the SCF domain, the PR errors for Z, H, C fall between 1% and 15%. In all the aforementioned cases, errors are relative to Span-Wagner EOS for fluid CO_2. The PR-EOS also seems adequate to describe the supercritical fluid (SCF) domain of CO_2 and its rich mixtures near critical transitions. This means that PR-EOS can be used to address any property (density, enthalpy, entropy, exergy, etc) of liquid and vapor phases of CO_2 and its mixtures with NG species under moderate errors, which are compatible with engineering applications (Li, 2008 and Li and Yan, 2009; Genesis, 2011). The PR-EOS is presented in Eq. (1), while its classical mixing rules follow in Eqs. (2) and (3). PR-EOS component parameters are given in Eq. (4) to (6) where Tc_i, Pc_i, ω_I and nc are, respectively, critical temperature, critical pressure, acentric factor for component i, and the number of components. K_{ij} represents the binary interaction parameter (BIP) for species i and j which is symmetric, can be used as zero in some cases, and is not necessary for pure CO_2. In Eqs. (1) to (3), V, T,P,R and N_i represent volume (m^3), temperature (K), pressure (bar), ideal gas constant ($8.314.10^{-5}$ bar.m^3/mol.K) and the mol number of species i.

$$P = \frac{NRT}{V - Nb} - \frac{N^2 a}{V^2 + UVNb + W(Nb)^2} \quad , \quad U = 2, \ \ W = -1 \tag{1}$$

$$Nb = \sum_{i=1}^{nc} N_i b_i \tag{2}$$

$$N^2 a = \sum_{i}^{nc} \sum_{j}^{nc} N_i N_j \sqrt{a_i} \sqrt{a_j} \sqrt{\Phi_i(T)} \sqrt{\Phi_j(T)} \left(1 - K_{ij}\right) \quad , \quad (K_{ij} = K_{ji}) \tag{3}$$

$$a_i = 0.45724 \frac{R^2 Tc_i^2}{Pc_i} \quad , \quad b_i = 0.07780 \frac{RTc_i}{Pc_i} \tag{4}$$

$$\Phi_i(T) = \left(1 + g(\omega_i)\left(1 - \sqrt{T/Tc_i}\right)\right)^2 \tag{5}$$

$$g(\omega_i) = 0.37464 + 1.54226\omega_i - 0.26992\omega_i^2 \tag{6}$$

If dimensionless terms in Eq. (7) are used in Eq. (1), the classic Z cubic form results in Eq. (8):

$$Z = \frac{PV}{NRT} \quad , \quad B = \frac{PNb}{NRT} \quad , \quad A = \frac{PN^2 a}{(NRT)^2} \tag{7}$$

$$Z^3 - (1 + B - UB)Z^2 + (A + WB^2 - UB - UB^2)Z - AB - WB^2 - WB^3 = 0 \qquad (8)$$

3. The CO$_2$ capture cycle

According to Oi (2010), CO$_2$ removal from process streams at an industrial scale has occurred since about 1930, mainly from natural gas and from industrial gases at high pressures for ammonia and methanol production. Like any separation unit in any kind of process, the CO$_2$ capture technology has to be judiciously chosen as it may undermine the profitability, controllability, safety, and simplicity of the plant. Nevertheless, even when properly selected, separations usually raise concerns like heat and mechanical energy consumption, increased utility use, carbon emission, chemicals demands, size, weight, footprint, construction re‐straints, operational hazards, etc.

The CO$_2$ capture cycle encompasses two or three main unit operations, which have to separate CO$_2$ from the gas mixture and send it to an appropriate destination. First, there is the CO$_2$ transfer across the gas phase into the medium that contains the binding material: a solvent or an adsorbent or a selective barrier. Second, there is (or not) the regeneration of the binding medium with concomitant CO$_2$ release. Third, there is the compression and cooling of the captured CO$_2$ because it has to be handled at high density or as a liquid.

Technologies for CO$_2$ capture from gas streams include chemical absorption (e.g., aqueous ethanolamines and aqueous K$_2$CO$_3$), physical absorption (e.g., propylene carbonate, selexol and rectisol), physical adsorption, membrane permeators, membrane contactors, cryogenic distillation and hybrid technologies (e.g., membrane permeator followed by ethanolamine absorption). Among those, the most relevant technologies include membrane permeation and chemical absorption with aqueous ethanolamines, the later standing as the most mature CO$_2$ capture technology from gas streams.

3.1. Chemical absorption with aqueous alkanolamines

With regards to the solvent, the advantages of the chemical absorption of acid gases – CO$_2$ and H$_2$S – by aqueous alkanolamines are well-known: the former are weak acids and the later are weak alkali, such that they reversibly bind at low temperature and high acid gas fugacity and subsequently untie at higher temperatures and low fugacity, leading to efficient acid gas stripping, which regenerates the solvent. The relevant variable in the liquid phase is the solvent loading (in mol of acid gas per mol of amine), which expresses the degree of conversion of amine in the solvent. Typically, the loading assumes values in the range 0 to 1.2 mol/mol amine.

AGWA (Acid Gas, Water and Amines) systems is a convenient denomination (de Medeiros et al., 2013a; de Medeiros et al., 2013b) of such reactive vapor-liquid equilibrium (RVLE) systems containing Acid Gas, Water and Amines. Amines are understood to be the common alkanol‐amines like monoethanolamine (MEA, MW=61), diethanolamine (DEA, MW=105), methyl‐diethanolamine (MDEA, MW=119) and 1-amino-2-propanol (AMP, MW=75).

MEA is a benchmark co-solvent for CO_2 capture, with: (i) satisfactory absorption capacity; (ii) fast kinetics; (iii) miscible with water in all proportions, and (iv) low cost. On the other hand, MEA is problematic in terms of solvent regeneration, because it exhibits: (i) the highest energy load per unit of stripped gas; (ii) corrosion and chemical/thermal degradation concerns; (iii) non-negligible evaporation losses due to its low boiling point; and (iv) high reactivity entailing low H_2S/CO_2 selectivity. As a secondary amine, DEA is less reactive than MEA but it has the following comparative advantages: (i) lower energy per unit of stripped gas; (ii) more resistant to degradation; (iii) less corrosive; and (iv) less volatile. MDEA exhibits the lowest reactivity with CO_2 and the greatest resistance to degradation. When compared to DEA and MEA, MDEA presents the following advantages: (i) the highest equilibrium capacity of acid gas absorption (in the case of CO_2, nearly two times the capacity of primary amine); (ii) lowest regeneration cost (does not form stable products with CO_2); (iii) high H_2S/CO_2 selectivity thanks to its low reactivity with CO_2; (iv) lowest enthalpies of reaction and lowest regeneration heat per unit of stripped gas; and (v) negligible losses due to very low vapor pressure. Alkanolamines with steric hindrance like AMP show reduced carbamate stability and the methyl adjacent to the amine group may affect absorption capacity and/or its rate. AMP exhibits absorption capacity and stripping heat similar to MDEA, but a faster reaction with CO_2 during the capture step (Medeiros et al., 2013b).

AGWA chemical reactions are really three-reactant transformations in the liquid phase with 1:1 amine to acid gas mol ratio. Water is necessary at high mol ratio to amine (8:1 or 7:1), otherwise the reaction simply does not evolve sufficiently, leaving non-solvated amine unconverted (low loading). This is the reason why MEA concentration in the solvent is upper bounded at 30%w/w in water (or 11.2%mol MEA + 88.8%mol H_2O), and 50%w/w in the case of MDEA (or 13.1%mol MDEA + 86.9%mol H_2O). Figure 6 presents a schematic of the chemical absorption system for CO_2/H_2S capture. AGWA absorption reactions take place in the colder higher pressure absorption column, whereas in the hotter lower pressure stripper column, AGWA reactions are reverted, thus releasing free acid gas and regenerating amine at the bottom. The main consumption of heat occurs in the reboiler in the bottom of the stripper column, where water is vaporized breaking the liquid phase association of acid gas, water and amine. Consequently, typical heat consumptions of MEA strippers lay between 167kJ and 200kJ per mol of stripped CO_2 (or between 3.8 GJ and 4.5 GJ/tonne of stripped CO_2). These figures are impressive high values, equaling 4 to 5 times the molar heat of vaporization of water per mol of stripped CO_2.

The literature presents several modeling approaches for absorption and stripping with AGWA systems. The most common approach involves cumulatively ionic species within ideal solution, ideal gas vapor phase, reversible chemical kinetics and rate-based interfacial mass transfer (de Medeiros et al., 2013b). This kind of approach is classical and is more adequate to low pressure and to dilute AGWA systems as in CO_2 capture from combustion gases. For high capacity and high pressure AGWA with rich CO_2 natural gas systems, high loadings and high heat effects may appear. For such AGWA systems de Medeiros et al. (2013a, 2013b) proposed a molecular Chemical Theory approach where molecular complex species are formed in the liquid phase via chemical equilibrium reactions having as reactants real AGWA species CO_2,
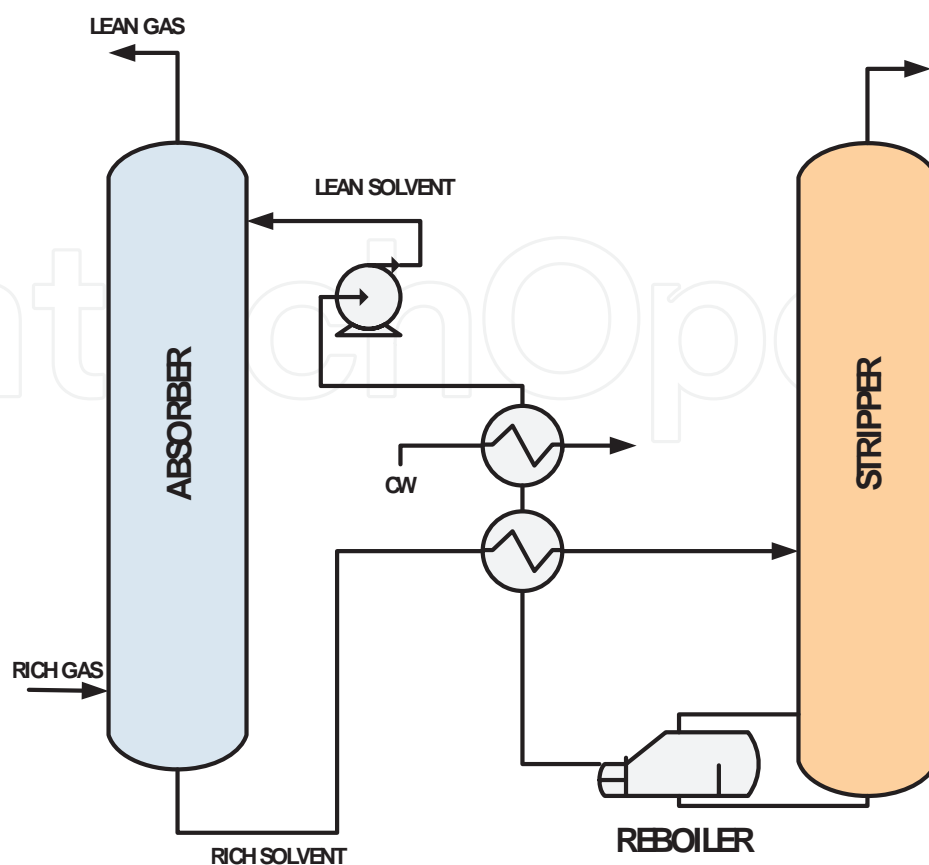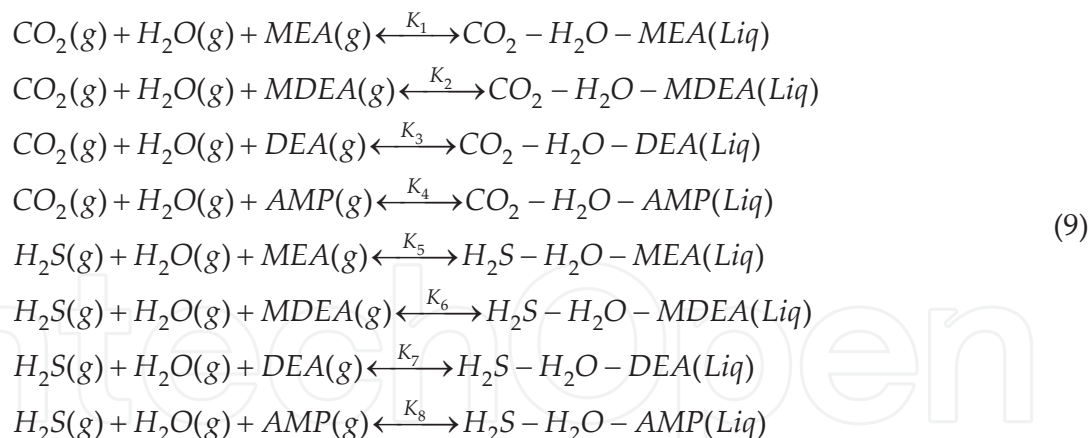
Figure 6. CO$_2$ capture by chemical absorption

H$_2$S, H$_2$O, MEA, DEA, MDEA and AMP. Each complex species is created by reacting three real species: an acid gas, water and an amine, as shown in Eq. (9). These complexes are reversibly created during the absorption step and destroyed during the stripping step. The main advantages of the molecular chemical theory of de Medeiros et al. (2013b) are:

i.   Theory is a Reactive Vapor-Liquid Equilibrium (RVLE) framework that employs only VLE AGWA data for model tuning via implicit statistical procedures. Model can be tuned with low or high pressure data, appropriate either for the absorption column (low temperature, high pressure) or for the stripping column (high temperature, low pressure).

ii.   AGWA RVLE is, in fact, an ionic scenario dominated by weak ions and several unknown solvated complexes. Thus, the limited knowledge to handle all the possible ions is circumvented via such nonionic, nonvolatile complexes.

iii.   Model tuning requires only AGWA VLE data, much more available than non-equilibrium counterparts.

iv.   The nonionic assumption is proposed to mimic the weakness of AGWA electrolytes, all created by incomplete dissociations.

v.   All thermodynamics properties (of both vapor and liquid phases) in the formalism of de Medeiros et al. (2013b) are calculated via cubic EOS (Soave-Redlich-Kwong - SRK and Peng-Robinson - PR), because all species considered are purely molecular.

vi.   The formalism can be used with both acid gases CO_2 and H_2S and with blends of alkanolamines, which are used for conjugating desirable qualities like good reactivity of MEA with lower costs of regeneration and corrosion of MDEA. Such blends are promising in terms of gains relatively to individual amines.

The AGWA formalism of de Medeiros et al. (2013b) was calibrated with VLE AGWA data from Literature. These data configure a large database of AGWA-VLE with 1331 runs shown in Figure 7. This database includes several runs with alkanolamines (MEA, DEA, MDEA and AMP), water and two acid gases or solutes (CO_2 and H_2S) at pressures ranging from 0.1 bar to 30 bar and temperatures from 25ºC to 140ºC. The calibration parameters correspond to chemical equilibrium constants belonging to chemical reactions that convert acid gas, water and amine into molecular complex species in liquid phase as shown in Eqs. (9). These chemical reactions are chemical equilibrium (ChE) reactions, which evolve to the right when CO_2 and H_2S are absorbed by the solvent and to the left when CO_2 and H_2S are stripped from the solvent by the action of heat and low pressure. In other words, the set of chemical equations in Eq. (9) can reproduce both phenomena absorption and solvent regeneration. This is a physically sound approach that allows, among other things, to estimate heat effects that occur in these processes like the release of heat during gas absorption and the absorption of heat during stripping of CO_2 and H_2S.

$$
\begin{aligned}
CO_2(g) + H_2O(g) + MEA(g) &\xleftrightarrow{\ K_1\ } CO_2 - H_2O - MEA(Liq) \\
CO_2(g) + H_2O(g) + MDEA(g) &\xleftrightarrow{\ K_2\ } CO_2 - H_2O - MDEA(Liq) \\
CO_2(g) + H_2O(g) + DEA(g) &\xleftrightarrow{\ K_3\ } CO_2 - H_2O - DEA(Liq) \\
CO_2(g) + H_2O(g) + AMP(g) &\xleftrightarrow{\ K_4\ } CO_2 - H_2O - AMP(Liq) \\
H_2S(g) + H_2O(g) + MEA(g) &\xleftrightarrow{\ K_5\ } H_2S - H_2O - MEA(Liq) \\
H_2S(g) + H_2O(g) + MDEA(g) &\xleftrightarrow{\ K_6\ } H_2S - H_2O - MDEA(Liq) \\
H_2S(g) + H_2O(g) + DEA(g) &\xleftrightarrow{\ K_7\ } H_2S - H_2O - DEA(Liq) \\
H_2S(g) + H_2O(g) + AMP(g) &\xleftrightarrow{\ K_8\ } H_2S - H_2O - AMP(Liq)
\end{aligned}
\tag{9}
$$

The parameter estimation of the AGWA model of de Medeiros et al. (2013b) involves estimating ChE constants for the chemical reactions in Eq. (9) at selected temperatures. Thus, several experimental AGWA VLE points at a chosen temperature are extracted from the AGWA database in Figure 7 and are processed via a maximum likelihood algorithm to estimate the ChE constants. The estimation algorithm also assures that the set of nonlinear constraints of each selected experiment is satisfied. The set of constraints of a given experiment is shown in Table 1 with Eqs. (10) to (16) including: (i) Real species – CO_2, H_2S, H_2O, MEA, DEA, MDEA, AMP – mass balance (RMB); (ii) mol fraction normalization for each phase (SXY); (iii) definition

partial pressures of solutes (acid gases) (PPS); (iv) definition of loadings of solutes (LDG); (v) VLE of Real species (VLE); (vi) ChE of Complex formation in Eq. (9) (CHE). The nomenclature used in Table 1 is shown in Table 2, including the matrix of stoichiometric coefficients of Eq. (9) in Eq. (10).
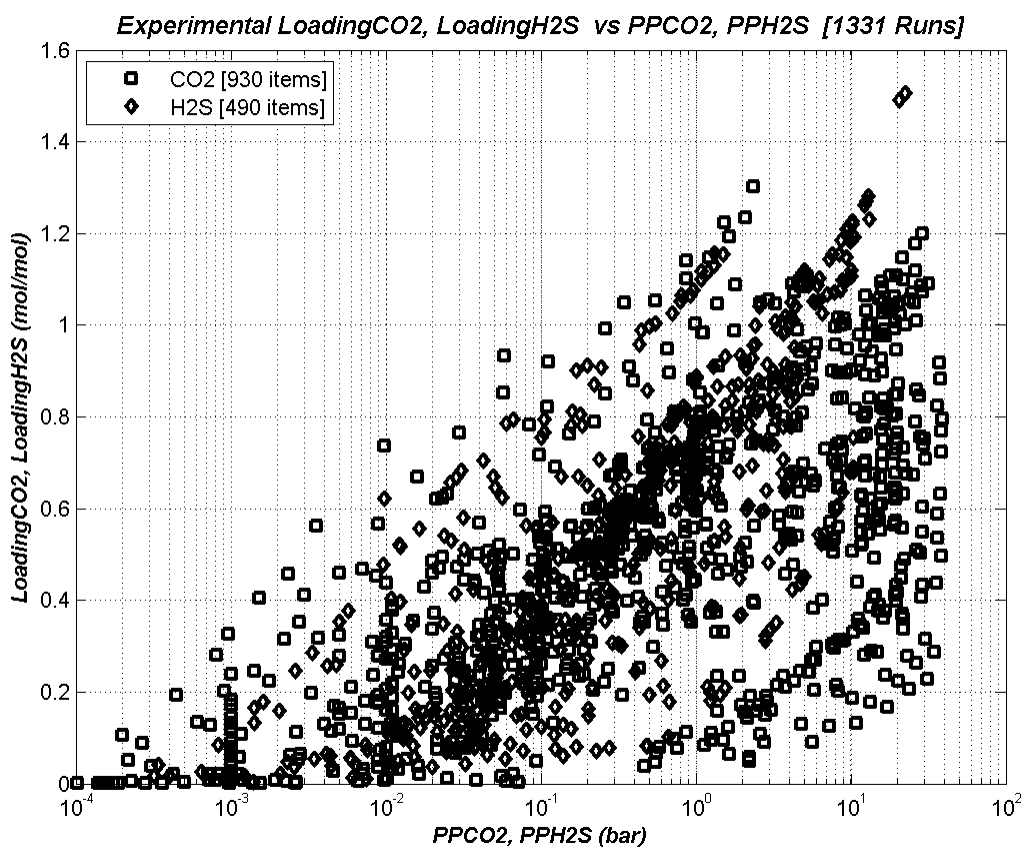

Figure 7. AGWA Database used to estimate parameters in the Chemical Theory Model of de Medeiros et al. (2013b) [PPCO2, PPH2S – partial pressures (bar) of CO_2 and H_2S]

Figures 8 and 9 depict some results after calibration of the AGWA model of de Medeiros et al. (2013b) with the database of AGWA experiments in Figure 7. Both figures refer to parameter estimation using 320 experimental AGWA data points at 40ºC. Figure 8 presents experimental versus predicted loadings (mol/mol amine) of solutes CO_2 and H_2S at 40ºC, whereas Figure 9 presents experimental versus predicted partial pressures (bar) of solutes CO_2 and H_2S at 40ºC. As can be observed, there is a satisfactory agreement between experimental values and predicted counterparts.

Predicted values are calculated solving the set of constraints of the AGWA model in Eqs. (I) to (VIII) with all thermodynamic properties (e.g. vapor and liquid fugacities) estimated with SRK-EOS. The estimated parameters are the eight ChE constants in Eq. (9) and (VIII) at the corresponding temperature of 40ºC.

Figure 8. Experimental vs predicted Loadings of CO_2 (blue) and H_2S (red) after calibrating the AGWA model at 40°C with 320 data points (de Medeiros et al., 2013b) [LdgCO2, LdgH2S – Loadings of CO_2 and H_2S (mol/mol amine)]
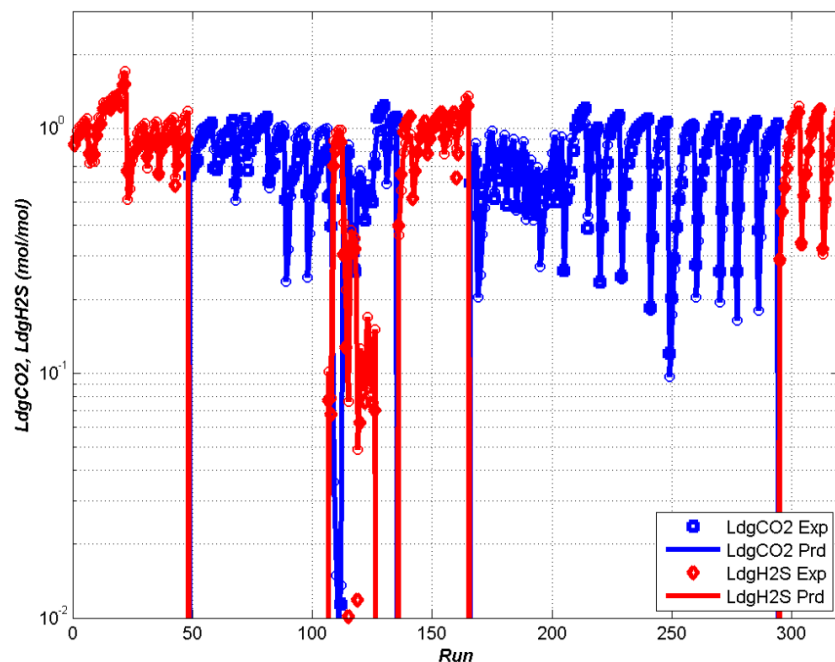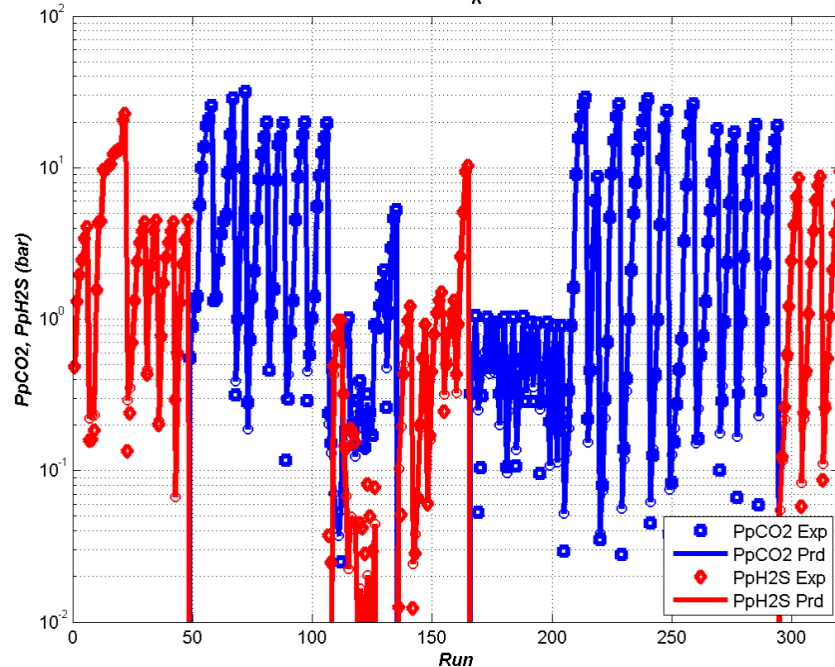

Figure 9. Experimental vs predicted partial pressures of CO_2 (blue) and H_2S (red) after calibrating the AGWA model at 40°C with 320 data points (de Medeiros et al., 2013b) [PpCO2, PpH2S – Partial pressures of CO_2 and H_2S (bar)]

Constraints [Label]	Expression	Eq.
n Real Species Balances [RMB]	$\underline{N} + L\underline{\underline{\Pi}}\,\underline{X}_C - L\underline{X} - V\underline{Y} = \underline{0}$	I
Normalizations [SXY]	$\sum\limits_{j=1}^{n} X_j + \sum\limits_{k=1}^{n_C} X_{Ck} - 1 = 0$	II
	$\sum\limits_{j=1}^{n} Y_j - 1 = 0$	III
n$_S$ Solute Partial Pressures [PPS]	$\underline{P}_S - P\underline{\underline{S}}_S\underline{Y} = \underline{0}$	V
n$_S$ Solute Loadings [LDG]	$(\underline{1}^T\underline{\underline{S}}_A\,\underline{N})\underline{\alpha}_S - \underline{\underline{S}}_S\left(\underline{N} - V\underline{Y}\right) = \underline{0}$	VI
n VLE of Real Species [VLE]	$\ln\hat{\underline{f}}^V - \ln\hat{\underline{f}}^L = \underline{0}$	VII
n$_r$ Reactions ChE [CHE]	$\ln\underline{X}_C + \underline{\underline{\Pi}}^T\ln\hat{\underline{f}}^L - \ln\underline{K}(T) = \underline{0}$	VIII

Table 1. Set of Constraints of AGWA VLE Experiments [real species (*n=7*): CO$_2$, H$_2$S, H$_2$O, MEA, DEA, MDEA, AMP], [solutes (*ns=2*): CO$_2$, H$_2$S], [Complexes (*nr=8*): see Eq. (9)]

Symbol	Definition
$\underline{\alpha}_S$	Vector of solute loadings (mol/mol of amine)
$\hat{\underline{f}}^V$, $\hat{\underline{f}}^L$	Vectors of Real species fugacities in vapor and liquid phases (bar)
$\underline{K}(T)$	Vector of ChE constants of Eq. (9)
L	Liquid phase mole number
n_S, n, n_r	Numbers of solutes (=2), Real species (=7) and Complex species (=8)
$\underline{N}$	Vector of total mole number of Real species in the experiment
$\underline{P}_S$	Vector of solute partial pressures (bar)
P	Pressure (bar)
$\underline{\underline{\Pi}}$	Matrix of stoichiometric coefficients of Eq. (9), shown in Eq. (17).
$\underline{\underline{S}}_A$, $\underline{\underline{S}}_S$	Selection matrices for amines and solutes with sizes 4 X 7 and 2 X 7
V	Vapor phase mole number
$\underline{X}, \underline{Y}$	Vectors of mol fractions of Real species in liquid and vapor phases
$\underline{X}_C$	Vector of mol fractions of Complex species in liquid phase

Table 2. Nomenclature used in Table 1

$$\underline{\underline{\Pi}} = \begin{bmatrix} -1 & -1 & -1 & -1 & 0 & 0 & 0 & 0 \\ 0 & 0 & 0 & 0 & -1 & -1 & -1 & -1 \\ -1 & -1 & -1 & -1 & -1 & -1 & -1 & -1 \\ -1 & 0 & 0 & 0 & -1 & 0 & 0 & 0 \\ 0 & -1 & 0 & 0 & 0 & -1 & 0 & 0 \\ 0 & 0 & -1 & 0 & 0 & 0 & -1 & 0 \\ 0 & 0 & 0 & -1 & 0 & 0 & 0 & -1 \end{bmatrix} \tag{10}$$

The huge heat consumption of MEA strippers (167 kJ to 200kJ/mol of stripped CO_2) forces investigation on more efficient alternatives of solvent regeneration. Wagener and Rochelle (2010) recognize as a "monumental task" reducing energy penalty of CO_2 capture from coal-fired power plants (approximately 30%). They presented an analysis of various stripper configurations, concluding that increasing complexity improves performance at the cost of higher capital and operational expenditures, i.e., an optimal scheme should exist. The alternative configurations include simple stripping with vapor recompression, multi-pressure, double matrix, split product, internal exchange, and flashing feed. Wagener and Rochelle (2010) concluded that operating with multiple pressure levels reduces the energy requirement as "equivalent work" (including reboiler duty, pumping and heat exchangers) in 33.6 kJ/molCO2 captured, with an optimal lean loading of 0.375 mol/mol amine. Moreover, they claim that the arrangement benefits from stripping at high pressure, whilst improves reversibility when returning to atmospheric conditions for the absorber. Wagner and Rochelle (2011) revisited several configurations with varying levels of complexity and reported that an inter-heated column and a simple stripper required 33.4 kJ/mol CO_2 and 35.0 kJ/mol CO_2 of equivalent work, respectively, at their optimum lean loadings.

3.2. Membrane permeators

The first membrane modules were developed as planar films. However, such arrangement has a low ratio of membrane transfer area per equipment volume. Presently, the majority of modules for CO_2 gas separation are manufactured in hollow-fiber or spiral wound configurations. Figure 10 shows a schematic of a hollow-fiber membrane permeator module and the selective transport of molecules across the hollow-fiber membrane.
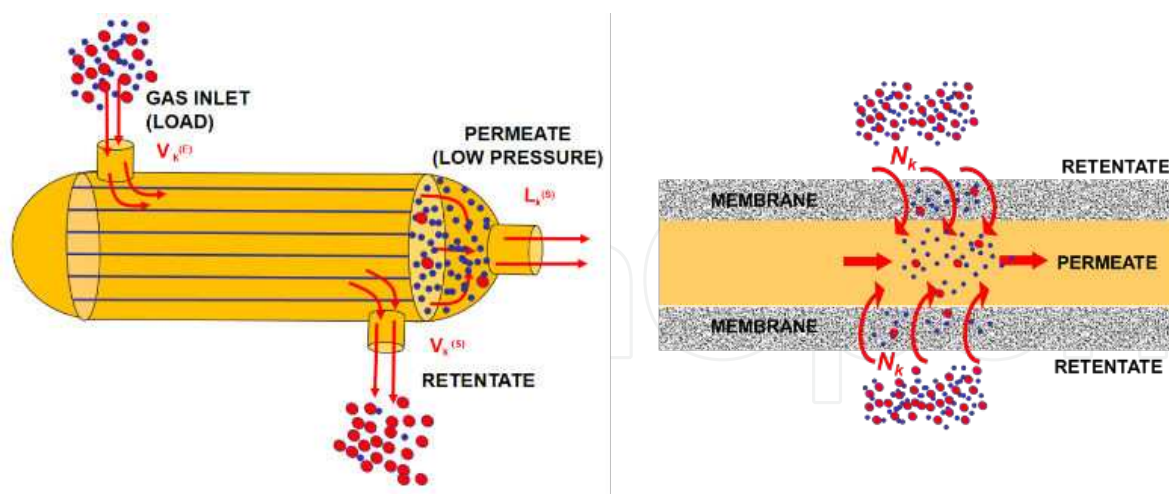
Figure 10. Hollow-fiber membrane permeator and the transfer through a hollow-fiber

The membrane acts selectively against gas diffusion from the high pressure side (the retentate) to the low pressure side (the permeate) creating separation. The membrane – either in hollow-fiber or spiral wound configurations – is composed by two polymeric structures: a permselective dense (nonporous) skin over a thicker microporous substrate. Inside the permeator gas

coming from the high pressure retentate stream solubilizes into the dense skin and diffuses to the low pressure side creating an almost adiabatic expansion with consequent fall of temperature via Joule-Thomson effect. Such fall of temperature may create problems to the proper functioning of the module due to eventual condensation of less volatile species that are retained and accumulate in the retentate. This condensation is undesirable and can damage the membrane plastic material.

Ho and Wiley (2005) evaluated the economic performance of membrane separation for low pressure (flue gas applications) and high pressure (e.g., natural gas processing). The authors concluded that the highest share in capital cost was due to the compression phase (around 80%) while membrane and the respective shells exhibited 10% of the investment. For natural gas processing, however, membrane has the largest share of CAPEX (about 62%), as the compression is an existing stage of natural gas processing. Moreover, Ho and Wiley also report an alternative multi-stage configuration in order to obtain a CO_2 rich permeate in a second membrane stage, which demands a recompression step corresponding to 30% of the total CAPEX.

In oil and natural gas deep-water offshore rigs, an issue in the processing of large volumes of NG with high CO_2/CH_4 ratio *vis-à-vis* climate concerns, involves large capacity CO_2 separators, whose targets are exportation of saleable NG from the retentate product via long pipelines and feeding enhanced oil recovery (EOR) systems with hyperpressurized CO_2 from the permeate product. In this scenario, robustness, angular indifference, modularity, and compactness also influence the selection of a separation technology. In this context, membrane permeation batteries are usually favored against the more traditional absorption columns with amine solvents (Medeiros et al., 2013a). On the other hand, large permeation batteries also have their own shortcomings, mostly related to the permselective dense (nonporous) skin over the microporous substrate. The permselective skin forces the existence of a high ΔP and exhibits low fluxes which means low capacity per unit area and high consumption of power for permeate recompression and/or permeate recycles. It also has CO_2/CH_4 limited selectivity and demands feed necessarily dew-point conditioned (to prevent gas condensation in the retentate provoked by the decrease of temperature associated with permeation) and continuous inspection looking for membrane bursts.

A model for hollow-fiber permeators can be built by writing mass, momentum and energy conservation principia for both permeate and retentate. Additionally, an appropriate model for trans-membrane flux transport is also necessary. Typically, trans-membrane flux models are written as products of a permeancy coefficient and a driving force term. Each species has a permeancy coefficient for a given membrane and given conditions of temperature, pressure and gas composition, but, in general, permeances are assumed independent of gas composition and pressure. The driving force term is usually expressed as a difference of component fugacities between the retentate and permeate sides. In this context and assuming a co-current compressible flow of both permeate and retentate, Nakao et al. (2009) proposed a stationary hollow-fiber membrane permeator rigorous model which can be used to predict CO_2 separation from CO_2 rich NG. The model of Nakao et al. (2009) builds a spatial 1-dimensional axial description where species mass balances, energy and momentum balances are rigorously

written for both permeate and retentate. All permeate and retentate thermodynamic properties (enthalpies, densities, fugacities, etc) are rigorously calculated via PR-EOS, Eq. (1). The model is too involved to be discussed here in detail, but the clarity and usefulness of it results are worth presenting in the context of CO_2 capture. Figure 11 depicts a natural gas feed named GBS2 (from Basin of Santos, Brazil) with 2.79554 $MMNm^3$/d at 53bar and 38°C with, initially, 25.32%mol CO_2 and 55.64%mol CH_4. Figure 11 depicts the VLE locus of GBS2 and the heat capacity (Cp in kJ/mol.K) map versus T X P with vivid identification of the critical and supercritical neighborhoods due to the second-order transition across the critical state that is revealed by second order properties like Cp. In Figure 11 [A], the gas feed is located at 28°C above its dew boundary (blue). GBS2 passes through a battery of 40 horizontal modules (0.2m X 10m each) of cellulose-acetate hollow-fibers (0.5mm ID), with CO_2 and CH_4 permeances respectively of $1.27.10^{-8}$ and $4.4.\ 10^{-10}$ $mol/s.m^2.Pa$ and $1854m^2$ of permeation area per module. Permeate pressure is 4bar and the external temperature is 27°C with a heat transfer coefficient of $5W/m^2.K$. Resulting profiles in the axial flow direction (10m long) for one module are shown in Figure 12. Permeate and retentate initiate contact at axial position $X=0m$ and cease contact at $X=10m$. The background along the axis of flow is painted in four colors for discrimination among the four quarters of a typical module. Figure 12 [A] depicts retentate profiles of %mol CO_2 and CH_4 showing a CO_2 decrease from 25.62% to 9.3%mol and a CH_4 increase from 55.64% to 65.5%mol. Figure 12 [B] shows that the final permeate recoveries of CO_2 and CH_4 are 72% and 11.5%. Figure 12 [C] depicts permeate and retentate temperature profiles revealing a drop of retentate temperature from 38°C to 29°C, insufficient for condensation (Figure 11 [A]).

3.3. Gas-liquid contactors

Gas–liquid contactors (GLC) constitute a new and versatile kind of membrane operation for CO_2 removal from NG. A GLC unit admits a gas stream which is contacted with a liquid stream (the solvent stream) through a polymeric micro-porous membrane. The solvent phase is an aqueous solution of ethanolamines (e.g. MEA and/or MDEA) that can absorb CO_2 as occurs in an absorption column. But the difference here is that the liquid and gas phases really do not mix as they do in direct contact devices like packing towers. Assuming that the GLC is manufactured with hollow-fiber membranes, the solvent phase flows in the hollow-fiber inner space while the gas phase flows in the outside shell space, but there are also configurations where the roles of liquid and gas phases are inverted. A module of hollow-fiber GLC with gas flowing in the shell side and with solvent flowing in the inner space of the hollow-fibers is sketched in Figure 13. As can be seen, the module resembles closely a shell and tube indirect contact heat exchanger.

GLC membrane operation can outperform common nonporous permeators in terms of capacity per unit area while sustaining high CO_2/CH_4 selectivity. High fluxes are possible in GLC because the membrane does not have a dense skin in order to be selective. The underlying reason is that selectivity is imposed by the solvent in the inner (permeate) side cutting the necessity of high ΔP across the membrane. As the reader can see, terms permeate and retentate are also used here despite some improperness, and refer, respectively, to the inner solvent flow and to the gas flow that was not transferred to the inner solvent.
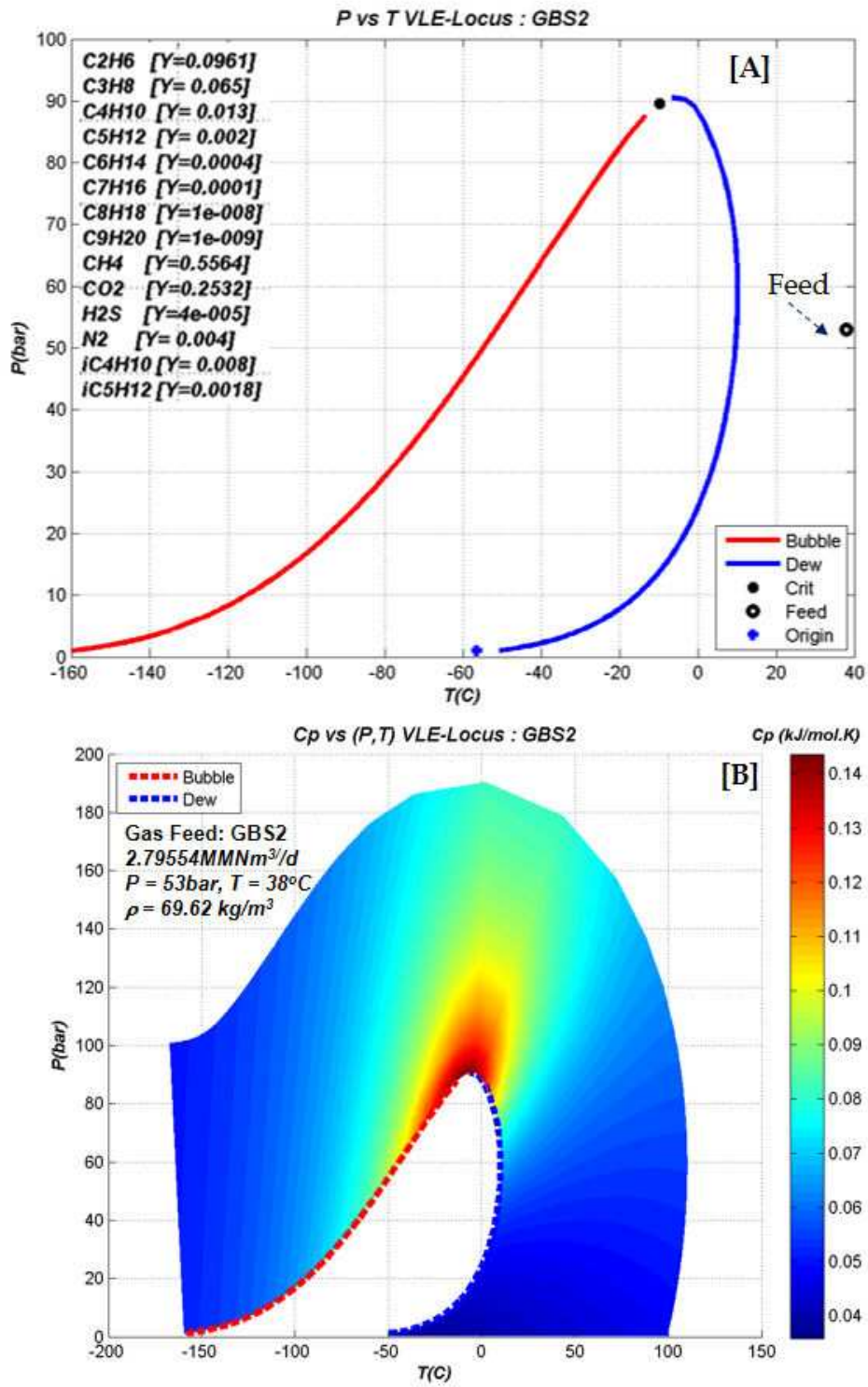
Figure 11. GBS2 a CO$_2$ rich natural gas (25.32%CO$_2$,55.64%CH$_4$,9.61%C$_2$H$_6$, 9.43%C$_3^+$) for Hollow-Fiber Permeator: [A] VLE Locus P(bar) X T(°C); [B] C_P(kJ/mol.K) vs P(bar) X T(°C)
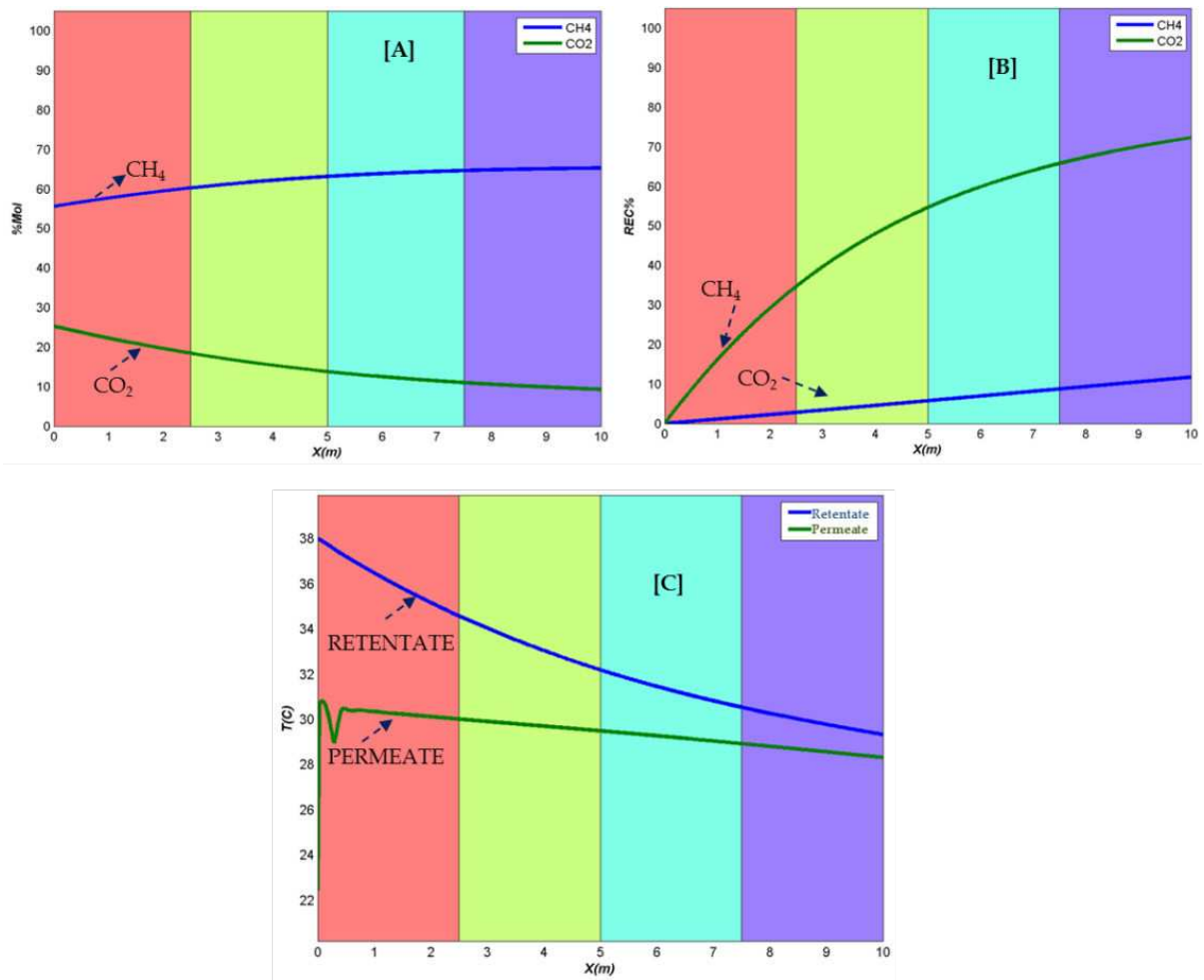
Figure 12. Profiles in a hollow-fiber module in co-current flow with feed GBS2 in Fig. 3.6 (25.32% CO_2 & 55.64% CH_4): [A] CO_2 & CH_4 %mol in retentate; [B] CO_2 & CH_4 permeate % recoveries; [C] retentate and permeate temperatures.
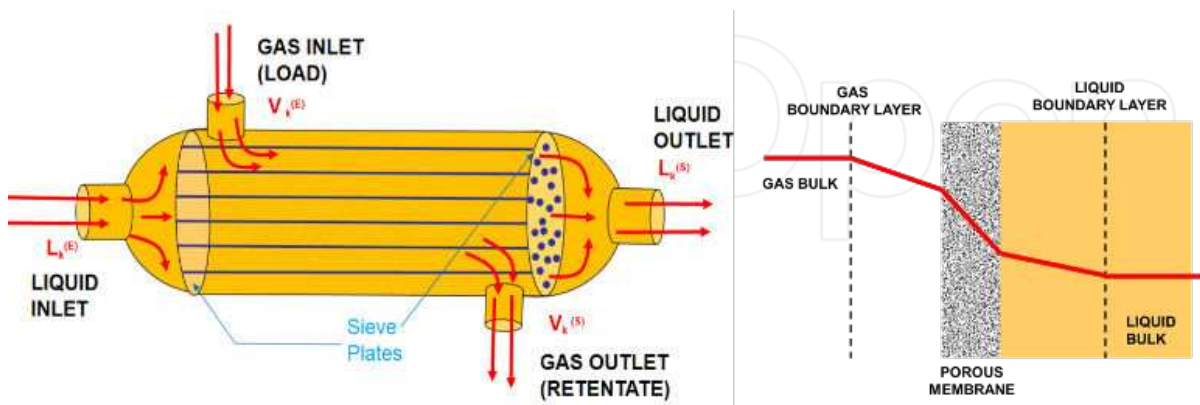
Figure 13. Hollow-fiber gas-liquid contactor with solvent in the inner space of membrane

GLC can separate CO_2 from NG offering the advantages of both membrane and absorption technologies, but leaving behind the respective shortcomings like the low flux coexisting with

high difference of pressure between the membrane sides and the flooding concerns coexisting with dependence on gravity in the case of absorption columns. GLC combines polymeric membrane separation and chemical absorption, using a physically and chemically active solvent for selective CO_2 removal. However, the new aspect is that there is a membrane standing as a physical barrier against the unnecessary mixing of gas and liquid phases. Other advantages of GLC are: (i) it allows independent manipulation of liquid and gas flows; (ii) offers larger area of gas–liquid interface; (iii) modularity ; (iv) it exhibits flexibility to increase/ decrease operational scales; (v) no dew-point conditioning of the gas feed is necessary; and (v) angular indifference allowing horizontal or vertical operational arrangements. Figure 14 sketches a typical process flowsheet for operation of a GLC unit capturing CO_2 from a NG feed.
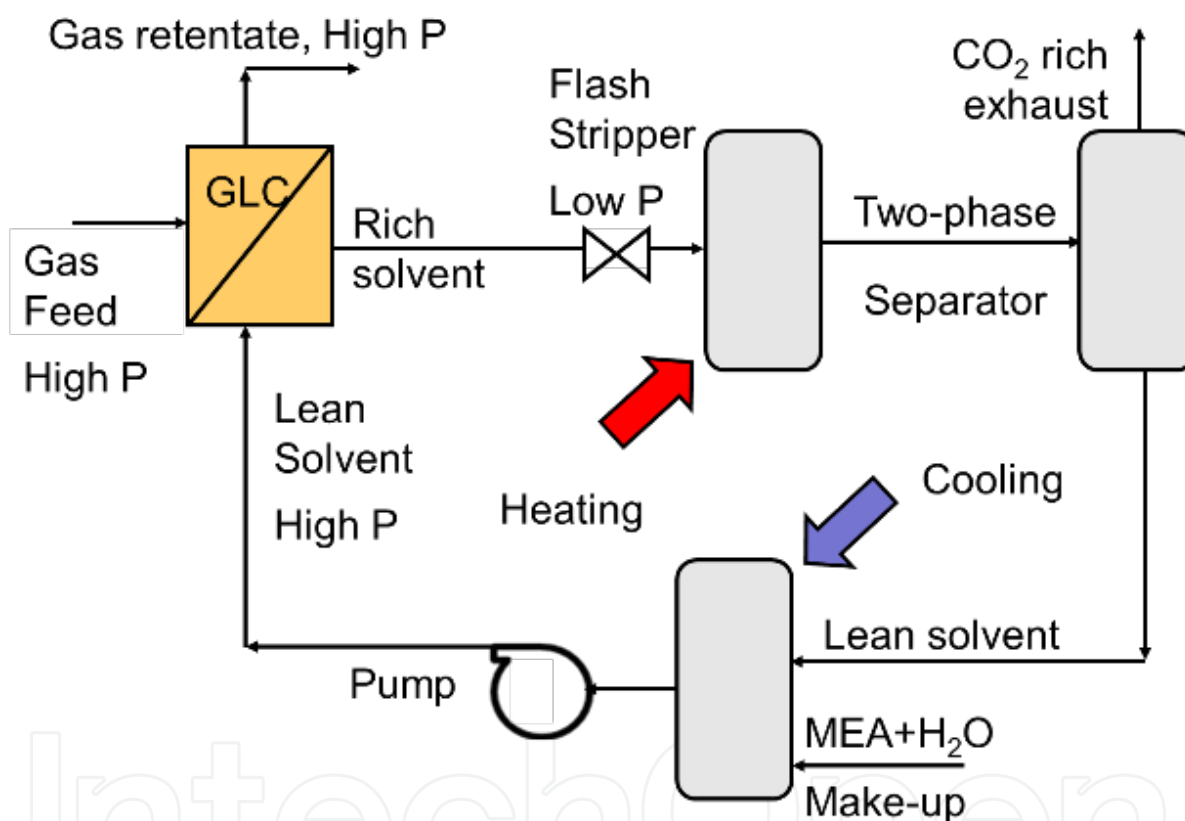
Figure 14. Typical process flowsheet for CO_2 capture with gas-liquid contactor (GLC)

Here the GLC operates t high NG pressure, but the rich solvent has to be regenerated in a low pressure stripper where CO_2 is released by the action of heating and low pressure as occurs in the second regeneration column shown in Figure 6.

A model for stationary gas-liquid hollow-fiber contactor was proposed by de Medeiros et al. (2013a) for separating CO_2 from CO_2 rich natural gas. This model is based on the AGWA theory discussed in the sub-section 3.1 (de Medeiros et al., 2013b). The model assumes a hollow-fiber contactor with co-current compressible flows of both permeate and retentate, where the permeate corresponds to the inner space inside the hollow-fibers. Permeate and retentate are

separated by the membrane. The permeate is supposed in two-phase flow because the trans-membrane flux of methane will support the maintenance of a gas phase in the inner permeate flow. The permeate is, in fact, a two-phase reactive flow in continuous reactive vapor-liquid equilibrium (RVLE) because CO_2 is in reactive vapor-liquid equilibrium with water and amine via a set of chemical equations similar to Eq. (9) (without the H_2S chemical equations if the GLC is designed for CO_2 capture only).

The model of de Medeiros et al. (2013a) is based on 1-dimensional axial geometry of the GLC. Species mass balances and momentum/energy balances are written for both RVLE permeate and gas retentate. All properties of gas and liquid phases are calculated with PR-EOS. The trans-membrane flux terms are written as products of permeancy coefficients and a driving force term. Each species has a permeancy coefficient for a given membrane and given temperature conditions. The driving force term is expressed as a difference of component fugacities between the retentate and RVLE permeate sides. The major difficulty encountered in the GLC model is to represent the RVLE two-phase flow in the inner membrane space. This is accomplished by solving the AGWA VLE model (de Medeiros et al., 2012b) described in Table 1, along the entire path of the permeate in the inner space of the hollow-fibers. As an example, consider the equilibrium map in Figure 15.

This map was calculated assuming that 1 mol of natural gas (with 16.7%mol CO_2 +82.3%mol CH_4) is contacted with 1.2 mol of liquid solvent containing 14.5%mol MEA +14.5%mol MDEA +71%mol H_2O. Only the chemical reactions of CO_2 absorption by MEA (Eq. 9a) and MDEA (Eq. 9b) are considered. Each point in Figure 15 represents the resulting equilibrium vapor phase mol fraction of CO_2 (Y_{CO2}) versus $T(^oC)$ X P (bar) under reactive VLE. Clearly, the locations with low Y_{CO2} (blue) are dominated by absorption phenomena, while those with high Y_{CO2} (red) are dominated by stripping phenomena. This kind of inner RVLE solver is a key element in the construction of the GLC model of de Medeiros et al. (2013a).

3.4. The CO_2 transportation cycle

An efficient and reliable transportation system is required to displace enormous quantities of captured CO_2 to their destination site at appropriate geological formations that are capable to accommodate hundreds of billions or trillions of Nm^3 of CO_2 under stable and secure conditions. Clearly a not especially large size thermoelectric coal plant can produce something like 1 million of metric tonnes (1Mt) of CO_2 per year or about $500.10^6 \ Nm^3/y$. Such huge capacities can only be attended by large pipeline systems operating with dense compressed fluid (liquid or dense supercritical CO_2), because the other existing alternatives – road, railroad and barge transport – simply cannot cope with dense fluid pipelines in terms of unitary cost and capacity of transportation.

In other words, despite of the existence of many options for transporting compressed (gas or liquid) CO_2 – including highway tankers, railway tankers, ships, and pipelines – it is evident that the impressive volumes that must be transported dictates that only pipelines working at high pressures, high densities and high capacities are suitable for this service. For instance, 2-3Mt/y of CO_2 have to be transported to dispose of the entire production of a single 500MW coal-fired power plant. This corresponds to transporting 230-350t/h of CO_2, just to service a

single, medium-sized, client. Thus, only a network of large-scale pipelines could provide viable overland transport of such massive flow rates of CO_2. Presently, about 50Mt/y of CO_2 (equivalent to the output of 16 coal-fired power plants) are transported by 3100km of CO_2 pipelines, mainly for EOR processes in the USA and Canada (de Medeiros et al., 2008). The best example is the 808 km long, 30" diameter, Cortez Pipeline that transports 13Mt/y of CO_2 from highlands in Colorado to oilfields in Texas, USA.
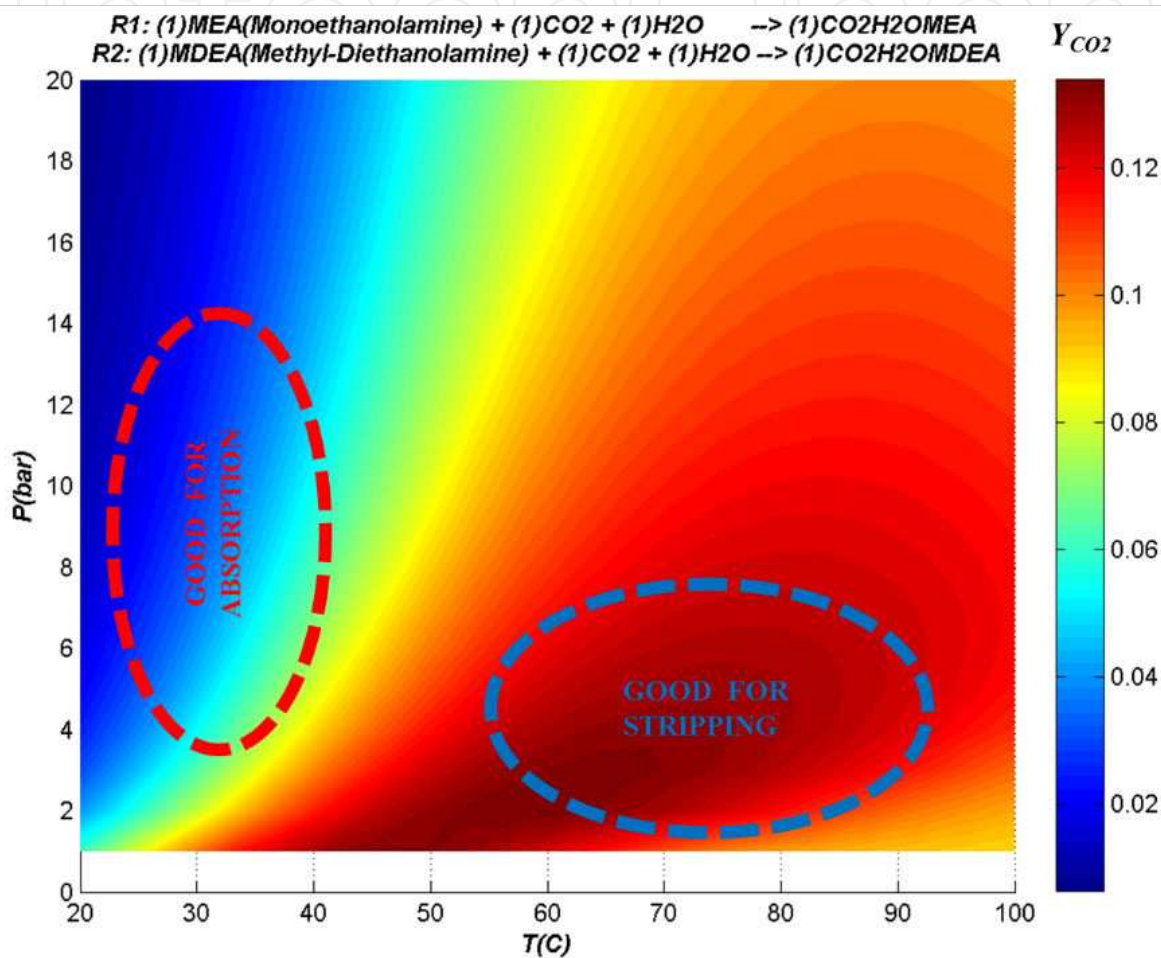
Figure 15. Equilibrium vapor phase mol fraction of CO_2 (Y_{CO2}) versus T(°C) X P (bar) under reactive VLE: 1mol of a 16.7%mol CO_2 natural gas is contacted with 1.2 mol of a liquid solvent with 14.5%mol MEA, 14.5%mol MDEA and 71%mol water.

Based on historical capital and O&M data for a 480-km long CO_2 pipeline without booster compressors, McCoy (2008) projected a fixed O&M coefficient of \$3,250/y/km for CO_2 pipelines. Considering a horizontal pipeline without appreciable elevation changes and an annualized fixed cost of 15% of capital, McCoy estimated the total unitary cost of CO_2 transportation as only \$1.16 per tonne of CO_2 per 100km. Based on a Monte Carlo sensitivity analysis, McCoy (2008) determined a range of \$0.75 to \$3.56 per tonne of CO_2 per 100km for this cost, recommending the median value of \$1.65 per tonne per 100km as a suitable estimate for investment decisions.

The design of CO_2 pipelines depends on reliable compressible flow models for dense compressible fluid near critical conditions. This model should account for thermal compressibility effects inside the fluid, i.e., temperature increases (decreases) during downhill (uphill) flow due to gravity compression (expansion).

In the same way, external heat transfer and elevation effects must be allowed. The extremely high compressibility of CO_2 near its critical state at 31°C (shown in Figures 4 and 5), leads to potential abrupt changes of velocity due to abrupt changes of density as the fluid compresses (decompresses) near the critical state. In other words, any candidate model for high capacity CO_2 pipelines must be able to calculate thermodynamic properties of dense supercritical CO_2 near its critical transition with accuracy. Such a CO_2 pipeline model has been proposed by de Medeiros et al. (2008) by solving rigorous species mass balances and energy/momentum balances along the pipeline with all thermodynamic properties given by PR – EOS or SRK – EOS.

This model is demonstrated in the simulation of a sub-sea CO_2 pipeline (Figures 16, 17 and 18) for transportation of 20 MMSm³/d of CO_2 from onshore plant to five EOR wellheads 2100m deep, 380km from the coast. The 20″ pipeline extends 380km from west to east and 320km from south to north with 700 km of length.
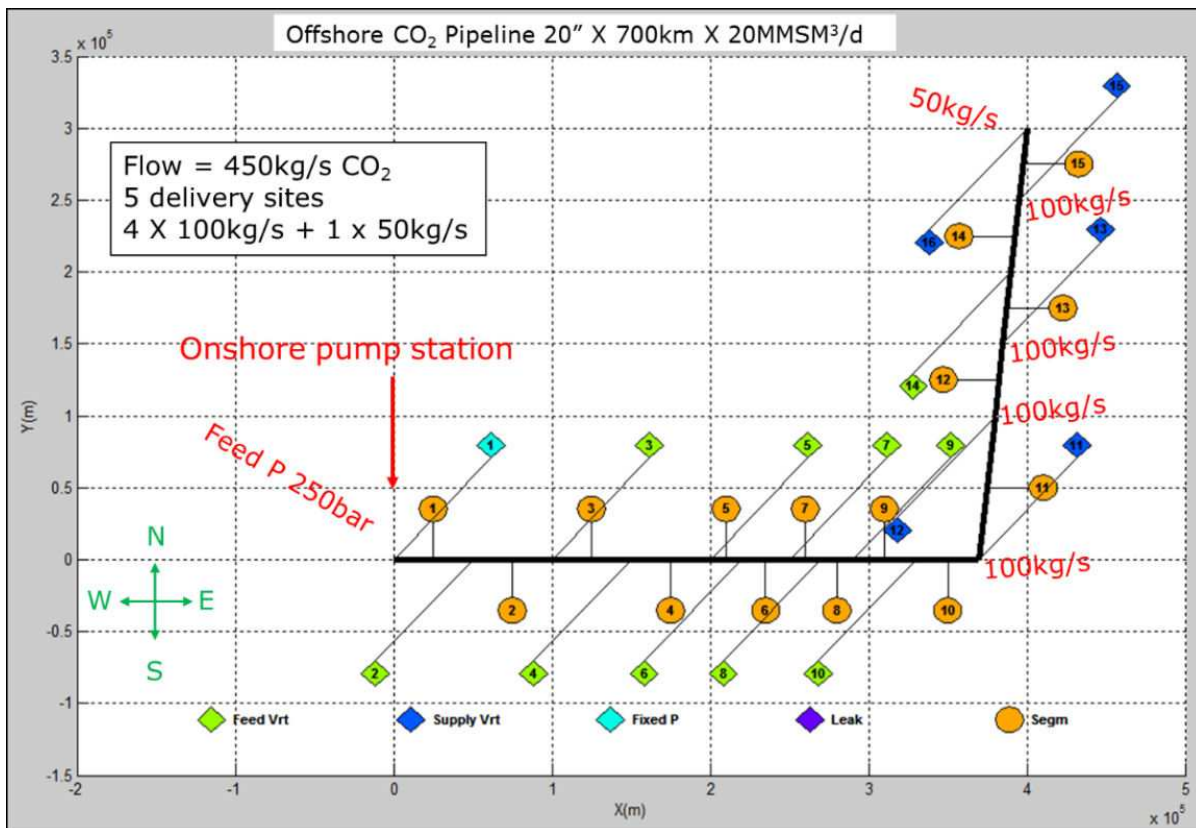
Figure 16. Hypothetical 20″X 700 km sub-sea pipeline for 20MMSm³/d of liquid CO_2 (≈450kg/s) at 250 bar from onshore plant to five offshore EOR wellheads (4X100kg/s + 1X50kg/s) 2100m deep, 380km from the coast.

As seen in Figure 17, a problematic factor was inserted between the continental shelf and the continental slope, namely, a big rift 1500m deep lies in the pipeline route. Rifts are not common in Santos Basin, Brazil, but they exist in the Norway arctic coast (Pettersen, 2011).
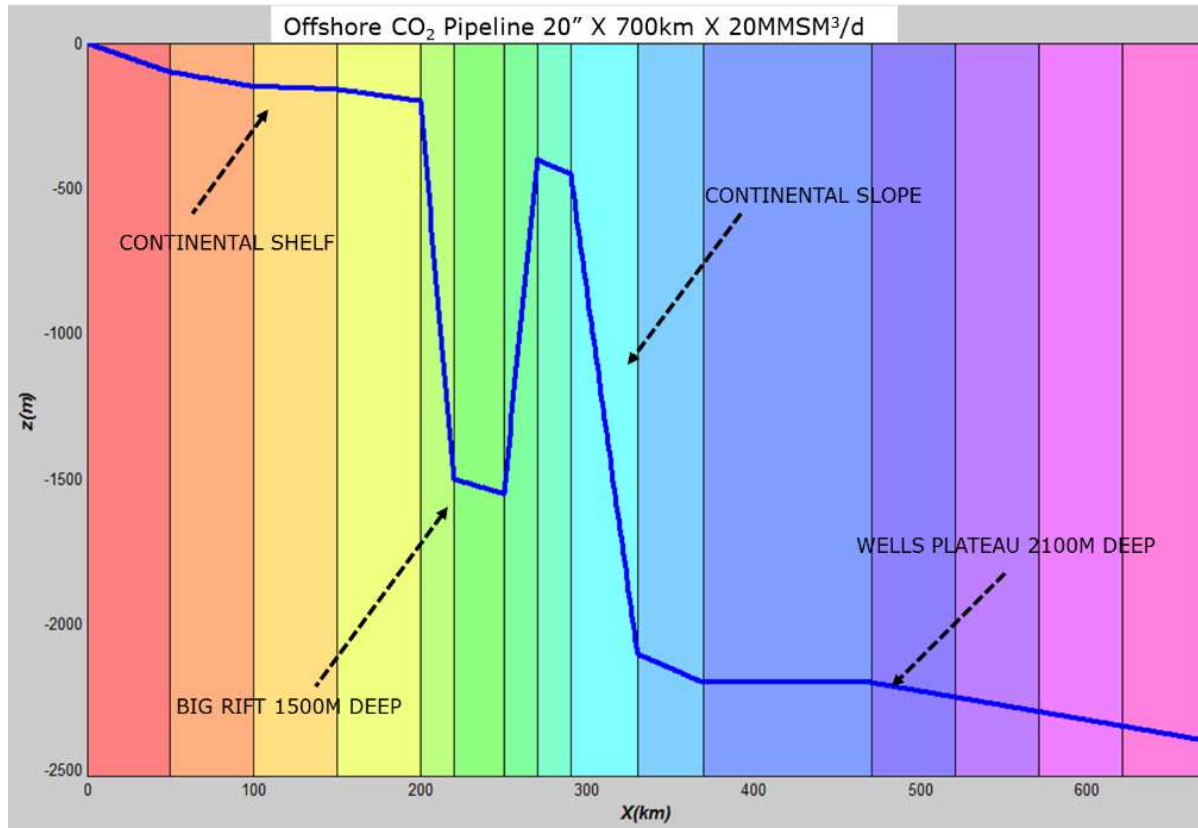
Figure 17. Elevation profile for the hypothetical sub-sea CO_2 pipeline from onshore plant to five EOR offshore well-heads 2100m deep, 380km from the coast.

4. The CO_2 utilization cycle

Although CGS has been regarded worldwide as a mitigation technology, it deals with CO_2 as a waste with an energy and an economic penalty for its disposal (Armstrong, 2012). Rather than treating CO_2 as a waste, carbon dioxide utilization (CDU) recognizes it as a raw material in chemical process to produce high added-value carbon containing products. It is also worth noting that the CDU is a complementary technology to CGS, not a competing technology, adding value to a process and thus it may help balance the costs of CGS.

While CO_2 has broad industrial application as solvent (supercritical CO_2, fire extinguishers) and in the food industry, it has disadvantages as a chemical raw material due to its low reactivity and few reactions are thermodynamically feasible. Furthermore, each potential use of CO_2 as reactant has an energy requirement that needs to be determined and must not exceed the CO_2 utilized and, although the utilization of CO_2 has been subject of research since before
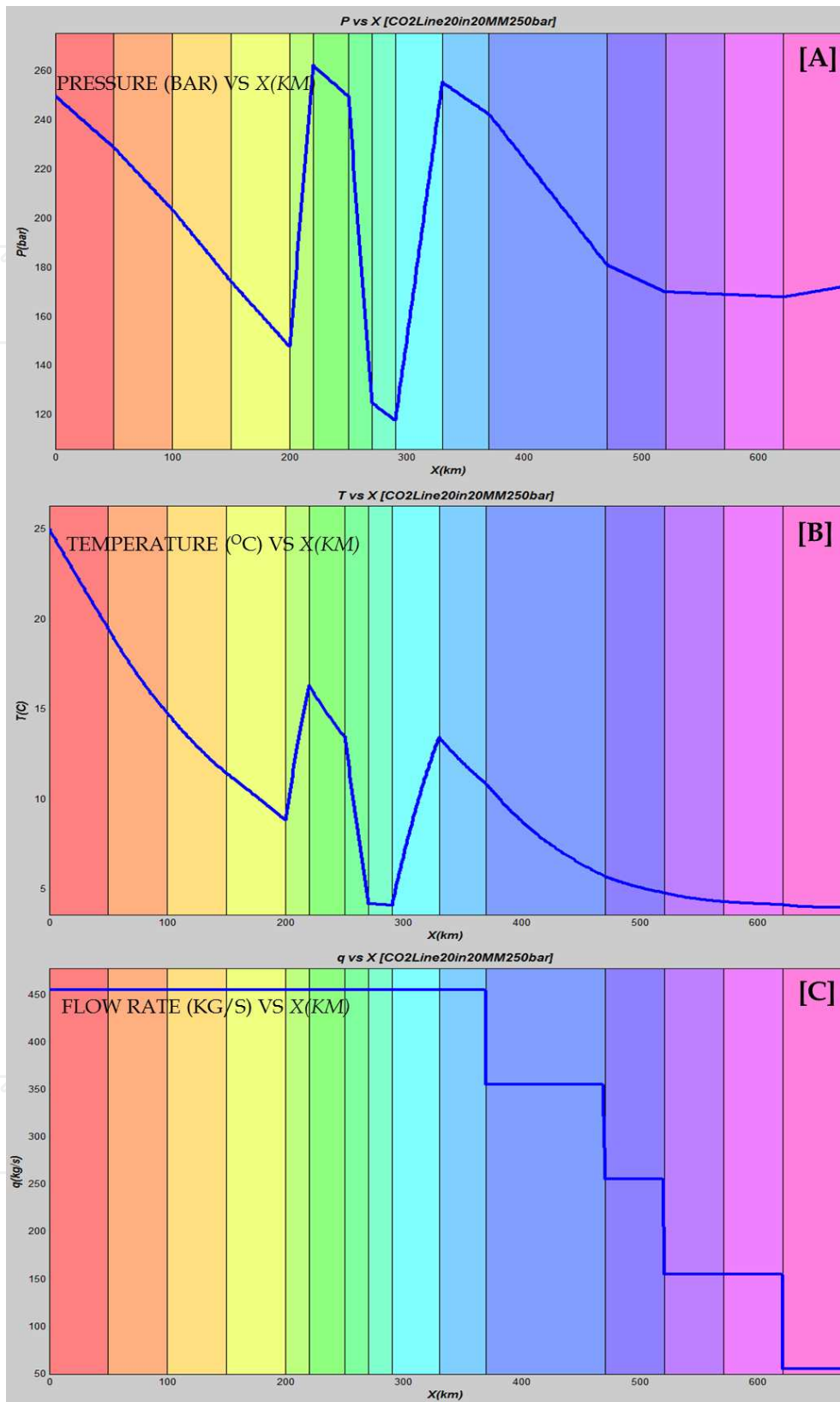
Figure 18. Calculated profiles for the hypothetical 20"X 700 km sub-sea pipeline with 20MMSm^3/d (≈ 450kg/s): [A] pressure (bar); [B] temperature (^{o}C); [C] mass flow rate (kg/s)

1970's, there is much research still needed for CO_2 activation. Moreover, the utilization of CO_2 to cause an effective reduction in its emission into the atmosphere, must observe certain guidelines (Aresta, 2010): (i) the new process must reduce the overall CO_2 emissions; (ii) it mustbe less energy - and material - intensive with respect to the on–stream processes that it aims to replace; (iii) the new process must reduce the overall CO_2 emissions; (iv) it must employ safer and more eco-friendly working conditions; (v) it needs to be able to operate on a commercial scale and (vi) it must be economically viable.
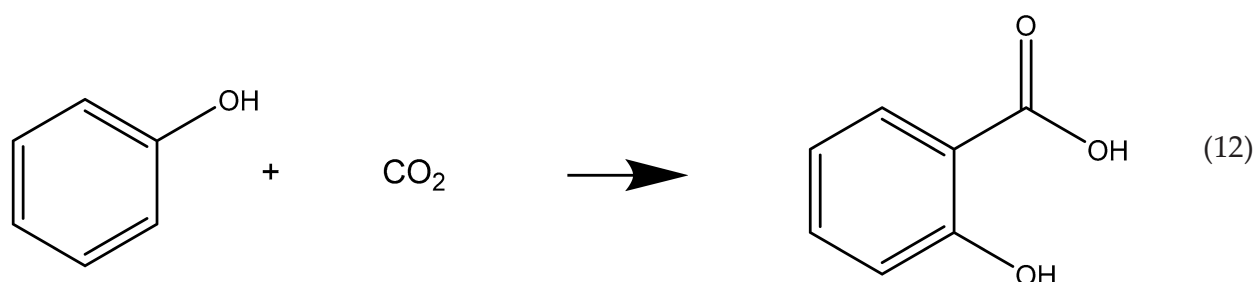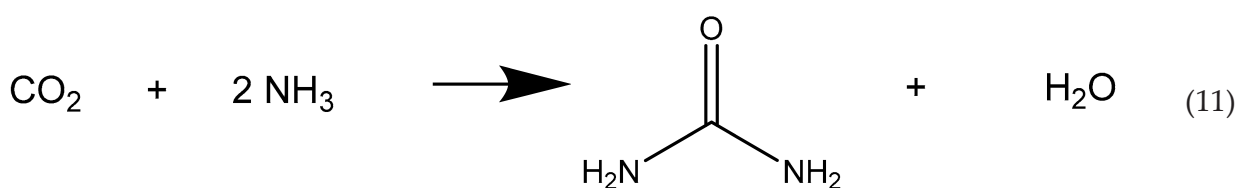
According to Song (2006), the global market for CO_2 is estimated to be $3.2 billion/year in 2003. Carbon markets across the world were valued at 96 billion euros ($122.28 billion) in 2011 (Reuters Agency, 2012). Utilization of CO_2 by the chemical industry exists for more than one century as, for instance, the synthesis of urea (50 Mt/y) (Aresta, 1999) (Eq. 11), salicylic acid (Song, 2006) (Eq. 12) and inorganic carbonates (20Mt/y) (Aresta, 1999).

$$CO_2 \quad + \quad 2\,NH_3 \quad \longrightarrow \quad \underset{H_2N \qquad NH_2}{\overset{O}{\|}} \quad + \quad H_2O \qquad (11)$$

$$\text{(phenol)} \quad + \quad CO_2 \quad \longrightarrow \quad \text{(salicylic acid)} \qquad (12)$$

According to Song (2006), the worldwide production of urea in 2002 was about 110 million metric tonnes, which contains 51.8 million metric tonnes of nitrogen with an estimated value of US$11.5 billion. This corresponds to about 81 million metric tons of CO_2, and 22 million metric tonnes of carbon.

4.1. Thermodynamic and chemical considerations of CO_2 conversion

Chemical reactions are driven by the difference in Gibbs free energy between the products and reactants at certain conditions. The obstacle for utilizing CO_2 as feedstock to industrial processes is its low energy level - CO_2 is a highly stable molecule. Consequently, a substantial input of energy, effective reaction conditions, and often catalysts, are necessary for its chemical conversion. In other words, many reactions for CO_2 conversion involve positive change in enthalpy, requiring an energy input. There are many large-scale chemical industrial processes that are operated based on endothermic reactions in the chemical industry (e.g., ammonia Haber process).

Song (2006) states properly that it is more energy-demanding if one were to use only CO_2 as a single reactant, but it becomes easier in thermodynamically terms if CO_2 is used as a co-reactant with another substance that has higher Gibbs free energy, such as CH_4, graphite and H_2. Song (2006) illustrates this trend by the change in the reaction heat for reactions with CO_2 as the single reactant (Eq. 13) and with CO_2 as a co-reactant (Eq. 14).

$$CO_2 \longrightarrow CO + \tfrac{1}{2} O_2 \qquad \Delta H^0 = +293 \, \frac{kJ}{mol\, CO_2} \tag{13}$$

$$CO_2 + H_2 \longrightarrow CO(g) + H_2O \qquad \Delta H^0 = +51 \, \frac{kJ}{mol\, CO_2} \tag{14}$$
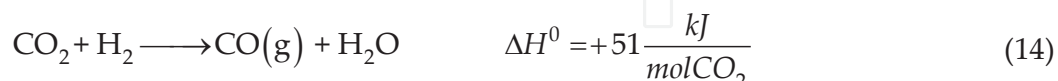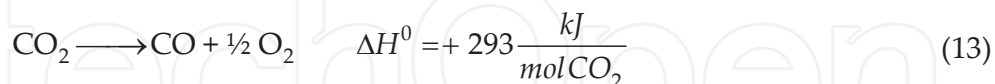
Therefore, energy input is necessary to transform CO_2 into chemicals. Four methods are possible: (i) reaction with high-energy molecules (e.g., ethylene oxide, H_2, unsaturated compounds and organometallic compounds); (ii) reaction with low energy oxidized compounds (e.g., organic carbonates), (iii) shifting chemical equilibrium towards products (via removal of a reaction product) and (iv) supplying physical energy (e.g., light or electricity) (Sakakura et al., 2007). The appropriate selection of chemical reactions makes it possible to obtain a negative Gibbs energy change.

As the carbon of the carbonyl group has an electron deficiency, CO_2 has great affinity for nucleophilic compounds and electron donors, i.e., as an anhydrous carboxylic acid, it promptly reacts with basic compounds. For instance, organometallic compounds, such as Grignard compounds, react promptly with CO_2 even at low temperatures. Reactions with CO_2 can be divided into two groups: (1) formation of a carboxylic group via a nucleophilic attack and (2) oxidative cycle addition yielding a ring of 5 members (Sakakura et al., 2007).

A relevant aspect to be considered is that utilization of CO_2 as feedstock does not necessarily contribute to the mitigation of greenhouse effects, even though CO_2 stands as a green reactant in many cases (Sakakura et al., 2007). Three points are hence relevant:

a. The chemical (or biochemical) fixation of CO_2 does not necessarily imply in reducing CO_2 emissions as its transformation requires energy, both to drive reaction (high temperatures and pressures) and separate products (separation occurs mainly at low pressures and, hence, recycling unreacted CO_2 to the reactor will require recompression at the expense of high energy input);

b. The energy demand of the world is order of magnitude higher than the amount of CO_2 fixed by chemical utilization of CO_2, and

c. In the critical phase of its life cycle, organic chemicals will emit CO_2. Nevertheless, the relevance of CO_2 as raw material stands for being a renewable feedstock, substituting the conventional fossil based routes

Among other utilization, CO_2 is currently used as supercritical solvent, refrigerant fluid, beverage carbonation agent, inert medium (such as fire extinguisher), pressurizing agent, neutralizing agent, gas for greenhouses, "inerting" applications to inhibit unintended chemical reactions, welding (preventing atmospheric oxygen from reacting with molten metal), food processing (suppressing aerobic bacterial activity for preservation in processes like pneumatic conveying or food storage). In any of these applications for inerting, carbon dioxide serves as a cover against atmospheric oxygen and is thus implicitly released into the atmosphere. The carbonation of beverages accounts for around 1.0×10^6 t CO_2/y. Nevertheless, they do not constitute CO_2 sink as it is ultimately released to the atmosphere or remains in a closed loop (Ormerod et al., 1995). Hence, this study does not review such utilizations.

4.2. Supply chain considerations of CO₂ conversion

Bayer (2013) estimates that the chemical industry has over 40,000 final chemicals, produced from approximately 400 intermediate chemicals, derived from ~40 basic chemicals that, in turn, are based on 4 classic feedstocks: petroleum, natural gas, coal and biomass. The Company expands the set of feedstock with the inclusion of CO_2.

For the near and middle term time-period, i.e., next one or two decades, it is reasonable to assume that presently dominant technologies (from an economic standing point) will persist and, consequently, expanding economies' demand of energy will be met by present technologies. Consequently, GHG emission of chemical processes will expand. This same approach leads to a transition scenario to a low-carbon economy equally dominated by presently installed infrastructure.

Hence, the CO_2 utilization cycle is likely to rely on commercially mature technologies or on technologies presently in large-scale pilot or demonstration plants as *Bridge Technologies*. Therefore, only peripheral technological advances are expected in these technologies such as process intensification, enhanced selectivity and activity of catalysts, and process optimization with increased mass and energy integration.

It is worth noting that 5 chemical commodities, ammonia, methanol, ethylene, propylene and BTX dominate energy consumption and GHG emissions in the chemical industry (IEA, 2013). In the conception of co-processing of fossil feedstock, with biomass and CO_2, conversion routes to produce ammonia, methanol and olefins (e.g., ethylene and propylene) are considered (Figure 2). Although not included in Figure 2, catalytic fast pyrolysis of biomass can lead to the key aromatic compounds, Benzene, Toluene, and Xylene (BTX), with generation of paraxylene from the BTX and subsequent conversion to Purified Terephthalic acid (PTA) and PolyEthylene Terephthalate (PET).

Synthesis gas (SYNGAS), a mixture of hydrogen, carbon monoxide and CO_2, is a versatile intermediate feedstock used in the production of a number of hydrocarbons such as methanol, ammonia, synthetic hydrocarbon liquids, and as a source of pure hydrogen and carbon monoxide. Applications of these products range from petrochemical feedstock to fuels.

According to Rostrup-Nielsen and Christiansen (2011), trends in the use of SYNGAS are dominated by the conversion of inexpensive remote natural gas into liquid fuels ("gas to

liquids" or "GTL") and by a possible role in a future "hydrogen economy" mainly associated with the use of fuel cells. Some relevant synthesis to the chemical industry are:

SYNGAS to Ammonia: Ammonia serves as a building block in many pharmaceuticals, fertilizers, ethanolamines, urea and cleaning products, as well as an anti-microbial agent in food processing. 50% of the world´s food production relies on ammonia fertilizers.

SYNGAS to Methanol: The main use for methanol is to produce other chemicals; about 40% is converted to formaldehyde, and further processed into plastics, plywood, paints, explosives and textiles. It is also used in anti-freeze, solvents, and fuels, and can serve as energy carrier.

SYNGAS to Hydrogen: Hydrogen generation is one of the largest energy-consuming steps in the production of the crucial chemical precursors of ammonia and methanol.

SYNGAS to Synthetic Fuels: Liquid hydrocarbons exhibit an excellent volumetric energy density and offer various opportunities for storing electric energy (Kaiser et al., 2013). Kaiser et al. (2013) point generation of SYNGAS by reverse water-gas shift (RWGS) at elevated temperatures as the first step, followed by Fischer-Tropsch (FT) synthesis. If CO is substituted by CO_2, less synthetic fuels are formed, the water-gas shift is repressed, and methane selectivity increases.

4.3. CO_2 to SYNGAS

SYNGAS is a toxic, colorless and odorless mixture. Its efficient commercial production is gaining significant attention worldwide (Raju et al., 2009) as it is a versatile feedstock to produce a variety of fuels and chemicals.

Almost any carbon source ranging from natural gas and oil products to coal and biomass can be used in the SYNGAS production. The lowest cost routes for its production, however, is natural gas (Spath and Dayton, 2003), which is also the cleanest of all fossil fuels. Furthermore, steam methane reforming is a well-established process for the production of SYNGAS and hydrogen (Gangadharan et al., 2012). The H_2/CO ratio varies over a wide range, depending on the primary feedstock and technology employed. Particular SYNGAS ratios are required depending on the chemical product desired, therefore creating flexibility for the chemical industry.

In the twofold context of avoiding emissions and standing as a renewable feedstock, carbon dioxide has been investigated as raw material in SYNGAS production. The new technologies involves CO_2: (i) reforming processes using a hydrocarbon (methane, typically) as reducing agent; (ii) using CO_2 as a co-reactant with hydrogen in the catalytic reverse water gas shift (RWGS); (iii) thermocatalytic (solar assisted) routes; (iv) electro- or photo-catalysis; (v) plasma processes, and (vi) bio-processes, e.g., by hybrid enzyme-nanoparticle systems, bioelectrochemical reduction or using a biomass char and a catalyst such as Ni/Al_2O_3.

CO_2 Reforming of CH_4 (Dry Reforming): The dry (carbon dioxide) reforming of methane has been of interest for a long time, dating back to as early as the 1920s, and was first proposed by Fischer and Tropsch (1928), but it is only in recent years that interest in it has rapidly increased for both environmental and commercial reasons (Zhang et al., 2003). Its name derives from the

fact that CO_2 replaces steam in the conventional steam methane reforming process (Hartley & Tam, 2012). This reaction can be represented as

$$CH_4 + CO_2 \longrightarrow 2CO + 2H_2 \qquad \Delta H = +247 \frac{kJ}{mol} \qquad (15)$$
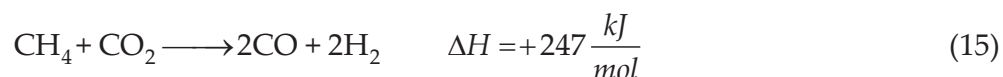
According to Hartley and Tam (2012), dry reforming utilizing CO_2 produces synthesis gas with higher purity and lower H_2/CO ratio than either partial oxidation or steam reforming. The produced SYNGAS has an H_2/CO ratio of unity without further post-reformer reactions (Zhang et al., 2003). The interest in this reforming route in recent years (Treacy and Ross, 2004, Shi et al., 2013) is due to two main reasons: (i) it produces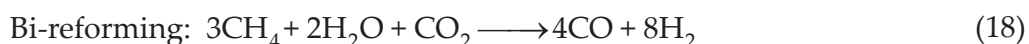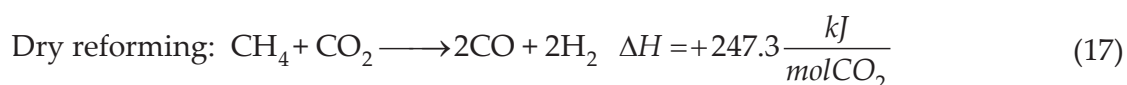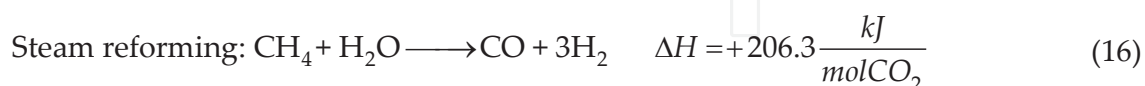 SYNGAS with a H_2/CO molar ratio that is suitable for a variety of products including Fischer–Tropsch fuels and (ii) the reaction consumes two types of greenhouse gases, CO_2 and CH_4 (Zhang et al., 2003, Gangadharan et al., 2012). Moreover, SYNGAS production stands as the most promising alternative of CO_2 utilization as it presents flexibility of using installed infrastructure to the manufacture of important chemical commodities.

The biggest limitation to the dry reforming process appears to be the availability of a suitable catalyst. The high temperatures required to reach high conversions, due to the endothermic nature of the process, contribute to carbon deposition (both CO_2 and CH_4 give off carbon deposits), and a catalyst capable of operating at such severely deactivating conditions has not been well developed (Zhang et al., 2003, Shi et al., 2013). According to Shi et al (2013), from the viewpoint of GTL industry, developing a catalyst for CO_2 reforming of CH_4 is a challenge, because the catalyst must exhibit very high production rates to render the GTL methane reformer as small as possible. Nevertheless, progress in the development of suitable catalysts with higher activities and optimized lifetime stabilities have been reported (Bradford and Vannice, 1999, Souza and Schmal, 2003; Zhang et al., 2003, Ginsburg et al., 2005; Kahle et al., 2013; Shi et al., 2013; Zheng et al., 2013; Edwards, 1995; Wurzel et al., 2000; Nagaoka et al., 2001; Li et al., 2004). Nevertheless, there is still no process for the CO_2 reforming currently considered to be commercially feasible. However, a variation of dry reforming has been used industrially (Hartley and Tam, 2012). The CALCOR process (Teuner, 1985, Kurz and Teuner, 1990, Teuner et al., 2001) involves dry reforming of methane, optimized to reduce the hydrogen content of the product gas. Furthermore, hydrogen separation by membrane permeators produces hydrogen gas that combusts a fuel (e.g., methane) producing pure carbon monoxide. The SPARG process (promotion by poisoning) is also a dry reforming reaction process (Gunardson, 1998; O'Connor and Ross, 1998; Rostrup-Nielsen, 2006). The active catalytic sites are blocked by poisoning the feed gas with hydrogen sulfide (H_2S). The adsorption of sulfur at the catalytic sites is favored over carbon growth. The SPARG process is claimed to produce high CO content SYNGAS.

Also combined CO_2 and steam reforming systems have been operational in the industry for a number of years (Gangadharan et al., 2012). By choosing the right proportions between CH_4, water and CO_2 (3/2/1), the combination of steam and dry reforming of methane can generate SYNGAS with a H_2/CO ratio of 2, ideal, for example, for the synthesis of methanol (Rostrup-

Nielsen and Christiansen, 2011; Olah et al., 2009). This combination of steam and dry reforming was named bi-reforming.

Bi-reforming could be advantageous in the use of various natural gas sources even these containing substantial amounts of CO_2. Some natural gas as well as biogas sources contain CO_2 concentration up to 50–70%. Bi-reforming can also be used to recycle CO_2 emissions from sources such as flue gases from fossil fuel (coal, petroleum, natural gas, etc.), burning power plants, exhaust of cement factories, among other industries (Olah et al., 2013). This reaction can be represented as

$$\text{Steam reforming: } CH_4 + H_2O \longrightarrow CO + 3H_2 \quad \Delta H = +206.3 \frac{kJ}{molCO_2} \tag{16}$$

$$\text{Dry reforming: } CH_4 + CO_2 \longrightarrow 2CO + 2H_2 \quad \Delta H = +247.3 \frac{kJ}{molCO_2} \tag{17}$$

$$\text{Bi-reforming: } 3CH_4 + 2H_2O + CO_2 \longrightarrow 4CO + 8H_2 \tag{18}$$

Bi-reforming is adaptable for reforming varied natural gas (containing hydrocarbon homologues) and CO_2 sources, e.g., shale gas (Olah et al., 2013):

$$3C_nH_{(2n+2)} + (3n\text{-}1)H_2O + CO_2 \longrightarrow (3n\text{+}1)CO + (6n\text{+}2)H_2 \tag{19}$$
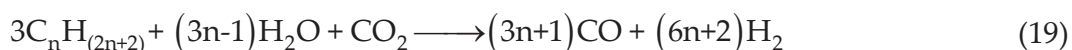
Numerous authors (Ashcroft et al., 1991; O´Connor and Ross, 1998; Wang et al, 200;, Jarungthammachote, 2011) have studied a similar idea, which combines dry reforming with partial oxidation. The idea again being that the combination helps overcome the endothermic requirement of dry reforming with the exothermic nature of partial oxidation, resulting in lower total energy consumption. In addition, it allows altering the H_2/CO ratio by controlling the extent to which each reaction takes place (Hartley and Tam, 2012). The combination of exothermic and endothermic reactions is called autothermal reaction (ATR). The ATR technology requires addition of CO_2 or CO_2-rich gas, in order to adjust the SYNGAS composition to the desired H_2/CO ratio.

$$\text{Dry reforming: } CH_4 + CO_2 \longrightarrow 2CO + 2H_2 \quad \Delta H = +247.3 \frac{kJ}{mol} \tag{20}$$

$$\text{Partial Oxidation of Methane: } CH_4 + 0.5O_2 \longrightarrow CO + 2H_2 \quad \Delta H = -35.6 \frac{kJ}{mol} \tag{21}$$
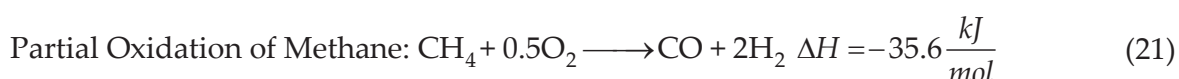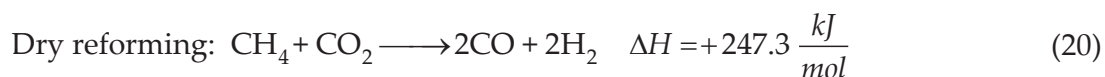
The combined Dry Reforming and Partial Oxidation is hence:

$$CH_4 + 0.5CO_2 + 0.25O_2 \longrightarrow 1.5CO + 2H_2 \quad \Delta H = +211.7\frac{kJ}{mol} \tag{22}$$
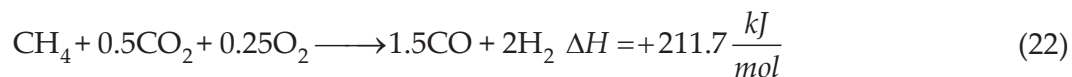
Integrating steam reforming and partial oxidation with CO_2 reforming could reduce or eliminate carbon formation on reforming catalyst, thus increasing catalyst life and process efficiency. Therefore, the tri-reforming, a synergetic combination of CO_2 reforming, steam reforming, and partial oxidation of methane in a single reactor for effective production of industrially useful SYNGAS (Song, 2006) could solve two important problems encountered in individual processing. Incorporating oxygen in the reaction generates heat *in situ* that could increase energy efficiency; oxygen also reduces or eliminates carbon formation on the reforming catalyst. The tri-reforming can be achieved with natural gas and flue gases using the waste heat in power plants and the heat generated *in situ* from oxidation with the oxygen that is present in flue gas (Zhou et al., 2008; Zangouei et al., 2010; Moon et al., 2004).

The tri-reforming process is presented in Eqs. (23) to (26) (Song and Pan, 2004):

$$\text{Steam reforming: } CH_4 + H_2O \longrightarrow CO + 3H_2 \quad \Delta H = +206.3\frac{kJ}{mol} \tag{23}$$

$$\text{Dry reforming: } CH_4 + CO_2 \longrightarrow 2CO + 2H_2 \quad \Delta H = +247.3\frac{kJ}{mol} \tag{24}$$

Partial Oxidation of Methane:

$$CH_4 + 0.5O_2 \longrightarrow CO_2 + 2H_2 \quad \Delta H = -35.6\frac{kJ}{mol} \tag{25}$$

$$CH_4 + 0.5O_2 \longrightarrow CO + 2H_2O \quad \Delta H = -880\frac{kJ}{mol} \tag{26}$$
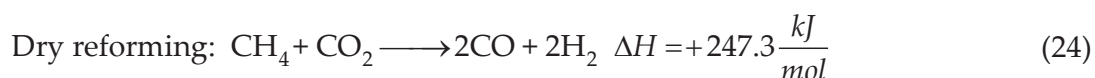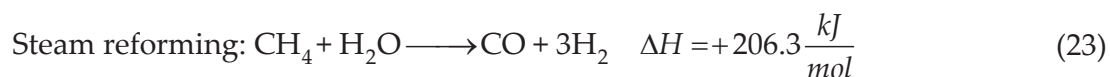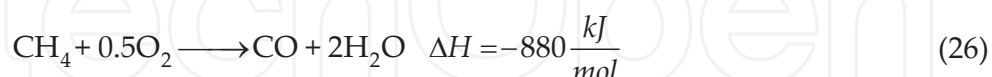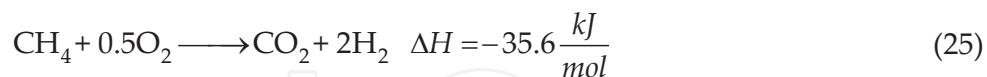
Song (2006) reports experimental and computational results to support that tri-reforming produces SYNGAS with desired H_2/CO ratios (1.5–2.0) and eliminates carbon formation in the CO_2 reforming of CH_4. Song (2006) suggests that tri-reforming is especially suited to using CO_2 in concentrated sources without prior CO_2 separation, as in non-conventional (low-quality CO_2-rich) natural gas, and has been demonstrated in pilot scale in Korea.

In general, produced SYNGAS from methane reforming is converted catalytically *in situ* via one of two main routes. The first is to use Fischer-Tropsch synthesis, a process that catalytically converts SYNGAS to hydrocarbons of varying molecular weights. The second is methanol

synthesis. The latter has better atomic economy, since the oxygen atom in CO is included in the product and CO_2 can be blended into SYNGAS as a reactant. However, production of methanol is very inefficient in this reaction: only 10-15% one pass conversion typically at 5.0-10.0 MPa and 523-573 K, due to the severe thermodynamic limitations of this exothermal reaction ($CO+2H_2 \rightarrow CH_3OH$) (Shi et al., 2013).

Finally, CO_2 reforming of methane can also be used as a chemical energy storage alternative and an energy transmission system (Richardson and Paripatyadar, 1990, Levitan et al., 1991; Levy et al., 1993). According to Zhang et al. (2003), in this system, solar energy is used to drive the endothermic forward reaction, and the energy thus stored can be transported via pipelines such as SYNGAS and liberated at will by the reverse reaction at any location or time. The highly endothermic reaction could be an option to store solar energy in hot regions (Zhang et al., 2013).

Reverse Water Gas-Shift (RWGS): The reverse water gas shift (RWGS) reaction has been known from over two centuries and is a well-researched and understood process for SYNGAS ratio alteration (Hartley and Tam, 2012). In fact, both the water gas shift (WGS) and the RWGS reactions are mostly used in combination with reforming of hydrocarbons to adjust the H_2/CO ratio, as shown in Eq. (27) (Song, 2006). Depending on the reaction conditions, the equilibrium for the WGS can be pushed in either the forward or the reverse direction. Efforts to explain the RWGS reaction mechanism are reported (Goguet et al., 2006, Meunier et al., 2007, Wang et al., 2013), and two main mechanisms have been proposed: the *redox* mechanism and the *associative formate* mechanism. The reversibility of the WGSR is important in the production of ammonia, methanol, and Fischer-Tropsch synthesis where the ratio of H_2/CO is critical. Many industrial companies exploit the RWGS reaction as a source of the synthetically valuable CO from cheap CO_2. In fact, catalytic RWGS reaction is the main route to produce SYNGAS from CO_2.

$$H_2 + CO_2 \longleftrightarrow CO + H_2O \quad \Delta H = +51 \frac{kJ}{mol} \tag{27}$$
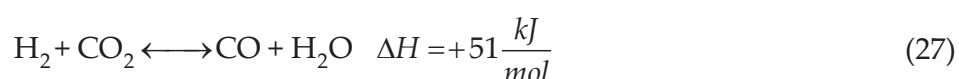
RWGS provides a source of hydrogen at the expense of carbon monoxide, which is important for the production of high purity hydrogen. This is a mildly endothermic reaction, as shown in Eq. (27).

Although high temperature reactions are effective for obtaining a high conversion, WGS reaction is an equilibrium-limited reaction that exhibits decreasing conversion with increasing temperature. In order to take advantage of both the thermodynamics and kinetics of the reaction, industrial scale WGS reaction is conducted in multiple adiabatic stages consisting of a high temperature shift (HTS) followed by a low temperature shift (LTS) with intersystem cooling (Byron, 2010). The initial HTS takes advantage of the high reaction rates, but is thermodynamically limited, which results in incomplete conversion of carbon monoxide and a 2-4% carbon monoxide exit composition. To shift the equilibrium towards hydrogen production, a subsequent low temperature shift reactor is employed to produce a carbon monoxide exit composition of less than 1% (Byron, 2010). A catalyst is required under these

conditions because of the lower reaction rate at low temperatures. The RWGS reaction uses a variety of catalysts, including palladium, platinum on titania, copper, cobalt with manganese/zinc oxide and rhodium with ceria (Tanaka et al., 2003, Saito and Murata, 2004, Meunier et al., 2007). Many research groups are looking at copper as a catalyst due to its effectiveness and its relatively low cost (Armstrong et al., 2013). However, there has been renewed interest in the WGSR at extreme temperatures, because of recent advances in high-temperature materials for hydrogen separation membranes (Bustamante et al., 2002).

4.4. CO₂ to methanol

Methanol is one of the most important commodity chemicals as it is used as a raw material in several intermediate chemicals and end uses. Methanol is produced industrially from SYN-GAS from natural gas or coal mainly containing CO, H_2 and a small amount of CO_2 in presence of a catalyst. Nevertheless, direct CO_2 hydrogenation has also been reported. Other non-conventional routes are electro- or photoprocesses, as well as the use of enzymes. The importance of methanol synthesis is demonstrated by widespread scientific publications of various reaction routes (Razali et al. 2012), and the development of several pilot plants to use waste carbon dioxide for methanol production.

Among the new technologies, in terms of potential for application, the CO_2 catalytic hydrogenation to methanol appears to have the highest degree of commercialization. It may be already commercially interesting when cheap sources of renewable H_2 are available, or to store excess electrical energy, as an alternative to actual systems. It is estimated that this reaction could reach the industrial stage in less than five years. This development would be pushed by experience in pilot or pre-commercial industrial plants, such as the Mitsui Chemicals Inc.'s plant (pilot in Japan capable of producing 100 t of methanol per year, and large unit expected in Singapore) and a plant by Carbon Recycling International (installed at the end of 2010) (Quadrelli et al., 2011). Mitsui's pilot plant uses CO_2 from an ethylene production plant of Osaka Works Petrochemical Complex (ADEME, 2010). It synthesizes methanol by CO_2 hydrogenation and the simultaneous water gas shift reactions. The process claims 96% selectivity (Hartley and Tam, 2009). Carbon Recycling International is capable of producing 3000 t/y of methanol (ADEME, 2010). This unit has a capacity of about 10 t of methanol from 18 t of CO_2 (Carbon Recycling International, 2009; Van-Dal and Bouallou, 2013), with CO_2 from the Svartsengi geothermal plant and an aluminum production plant. Hydrogen is generated from the electrolysis of water using a renewable source of electricity.

Methanol from SYNGAS: Synthesis gas composed of the proper ratio of hydrogen, carbon monoxide and carbon dioxide is converted to methanol. Alternatives paths to methanol are via CO from RWGS reacting with hydrogen according to Eq. (28) and via CO_2 being hydrogenated following Eq. (29).

$$CO + 2\,H_2 \longrightarrow CH_3OH \qquad \Delta H = -90.6\,\frac{kJ}{mol} \qquad (28)$$

$$CO_2 + 3\,H_2 \longrightarrow CH_3OH + H_2O \quad \Delta H = -49.5\,\frac{kJ}{mol} \qquad (29)$$
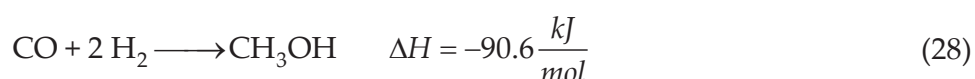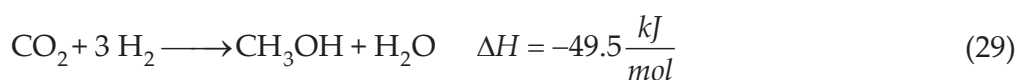
From Eq. (28), production of methanol involves SYNGAS production as intermediate stage. Hence, two steps are required for the manufacture of methanol: reduction to SYNGAS and reaction to form methanol. There are process variations for implementing the sequence. Before being sent to the methanol production unit, the SYNGAS must thus be subjected to the WGS reaction to enhance its hydrogen content. Alternatively, H_2 from other sources can be added. Recent efforts have been aimed at production of methanol in a one-step process without intermediate formation of SYNGAS. Homogeneous or heterogeneous catalysts are typically preferable. The conventional process occurs at relatively low pressures (5 to 10 MPa) and 210 to 350 °C employing a $Cu/ZnO/Al_2O_3$ catalyst.

Catalytic Hydrogenation Conversion of Carbon Dioxide to Methanol: The most direct and studied route to methanol from CO_2 is the catalytic conversion of CO_2 with hydrogen. Carbon dioxide hydrogenation to methanol is a relatively mature process. The main issue is the cost (and associated carbon footprint) of the H_2 necessary for the reaction. Any available energy source (alternative energies such as solar, wind, geothermal, and atomic energy) can be used for the production of needed hydrogen and chemical conversion of CO_2. The process can use lower operational pressures of 3 MPa at 240 °C. This direct CO_2 hydrogenation exhibits low conversions resulting in high volumes of recycled gas. Literature indicates that methanol is synthesized following a 3:1 hydrogen to carbon dioxide stoichiometry using catalysts of copper oxide, zinc oxide, incorporating either titania, aluminum oxide, chromium oxide and alternatively lanthanum or gallinium (Lachowska and Skrzypek, 2004, Lee et al., 2004, Stoczynski et al., 2004).

An alternative approach to the use of solid catalysts and a gas phase process is to employ the so called low-temperature methanol synthesis (LTMS) (Dixneuf, 2011). LTMS is based on the catalytic hydrogenation of methanol to formic acid (HCOOH) with subsequent etherification to methanol formate (alternative to methyl formate from SYNGAS), followed by hydrogenation of formate to two methanol molecules using Pincer-type ruthenium(II) catalyst (Balaraman et al, 2011; Dixneuf, 2011; Huff and Sanford, 2011). A liquid-phase allows CO_2 and H_2 conversion to methanol of about 95% with very high selectivity in a single pass (Olah, 2009). Waugh (2012) has published a review on catalytic methanol synthesis which includes the use of carbon dioxide as a feedstock.

Photoreduction of CO_2 to methanol: Photoelectrochemical reduction of carbon dioxide or photocatalysis generally uses semiconductors to promote reaction in the presence of sun light. The semiconductor is used as a catalyst to absorb solar energy and generate electrons and protons needed for the reduction of carbon dioxide. While hydrogenation of carbon dioxide requires high temperature and high pressure conditions, photocatalysis carries out under relatively mild conditions with advantageous energy input – sun light – a continuous and readily available source (Le, 2009).

Considerable research effort has been made on CO_2 activation by visible light photocatalysts due to the natural abundance of sunlight. Nevertheless, the efficient photoreduction of CO_2 with H_2O remains one of the most challenging tasks of environmental catalysis.

CO_2 can be reduced in water vapor or solvent by photocatalysts such as TiO_2 and ZnS. Eq. (30) describes the overall reaction.

$$CO_2 + 2H_2O \xrightarrow{\ h\nu\ } CH_3OH + 3/2\ O_2 \qquad (30)$$

Due to the high energy requirements, this method is often combined with electrochemical methods via photoelectrocatalysis to drive the reaction (Hu et al., 2013). The catalysts traditionally used are transition metal complexes, TiO_2, ZnO, CdS, and functionalized metal surfaces (Yamashita et al., 1998; Kuwabata et al., 1994). A wide variety of CO_2 photoreduction has been achieved on the surface of TiO_2 under UV irradiation. The yield of photoproducts can be changed substantially under different experimental conditions such as UV wavelength, UV intensity, additives of reaction media and reactor configuration. Other variables, such as CO_2 pressure, moisture and residence time are also important in photoreducing CO_2 (Wu & Lin, 2005).

Electrochemical Production of Methanol from CO_2 and H_2O: The direct reduction of CO_2 to CH_3OH is known to occur at several types of electrocatalysts including oxidized Cu electrodes. The current stage of the technology is still very experimental. The majority of tests have been performed on a laboratory scale with a purpose of either kinetic analysis or proof-of-concept to examine product distribution for different material and condition combinations (Beck et al., 2010). An advantage of electrochemical CO_2 reduction is that unlike many other hydrocarbon processes it can occur at ambient conditions.

The electrochemical reduction of carbon dioxide to methanol is thermodynamically possible, but there seems to be no well-established technique to achieve this reaction with high current efficiencies close to l00%. Nevertheless, methanol production has been reported with the use of ruthenium: gallium arsenide and RuO_2-TiO_2 mixed cathodes (Le, 2009). Cole and Bocarsly (2010) have reviewed electrochemical reduction processes, including electrochemical CO_2 conversion to methanol. Few studies have investigated the feasibility of this technology, and none has been found to provide an in-depth analysis of its potential industrial implementation.

Applications of Methanol: Methanol has traditionally been used as feed for production of a range of chemicals including acetic acid, formaldehyde and MTBE (Olah, 2009). In recent years, methanol has also been used for other markets such as production of Di-methyl-ether (DME) and olefins by the so-called methanol to olefins process (MTO) or as blendstock for motor fuels. As a liquid fuel, methanol is of interest especially for use in fuel cells (Olah, 2009).

Methanol to Olefins (MTO) explores alternative pathways to produce small olefins, in particular ethylene and propylene. Conventional steam cracker feeds are either natural gas liquids (NGL) or heavy liquids (i.e., naphtha). Ethane cracking, however, is increasing its share as feedstock. A promising alternative route is dehydration of methanol (MTO). Methanol-to-

olefins (MTO) was first developed by ExxonMobil (1980s) as part of its methanol-to-gasoline (MTG) process. In the 1990s, UOP and Norsk Hydro built an MTO pilot plant in Norway. Since then, Lurgi has developed its own version of this process, methanol-to-propylene (MTP).

4.5. CO_2 to DMC

Dimethyl carbonate (DMC) is a biodegradable and nontoxic chemical acceptable environmentally as a chemical destination of CO_2. It is exempted from VOC classification and can be used as raw material for producing valuable chemicals, including aromatic polycarbonate, and qualifies as an octane booster component in gasoline and diesel. It is a safer and nontoxic substitute of well-established methylating-carbonylating hazardous chemicals like dimethyl sulfate and phosgene (Souza et al., 2013). Although DMC is presently produced on a relatively small scale, approximately 400 kt/y, its demand has grown strongly in recent times because of its green properties.

Currently, DMC is produced mainly by oxidative carbonylation of methanol (Aoussi et al., 2010). The direct methylation reaction is possible where, according to Ferreira et al. (2013), the most used catalyst is tin, employed as an oxide compound or as an organometallic complex, according to Eq. (31):

$$2\ CH_3OH \quad + \quad CO_2 \quad \longrightarrow \quad DMC \quad + \quad H_2O \tag{31}$$

However, direct methylation presents low yields, inferior to 10%, due to the chemical inertness of CO_2 and to the deactivation of catalysts induced by water formation in the reaction (Aouissi, 2010). For large-scale production of DMC from CO_2, one route seems to be promising: the indirect route (IR) for two-step conversion of CO_2 with ethylene oxide (EO) to ethylene carbonate (EC), which then reacts with excess methanol (MeOH) giving DMC and ethylene glycol (EG) as shown in Eqs. (32) and (33).

$$EO \quad + \quad CO_2 \quad \longrightarrow \quad EC \tag{32}$$

$$\text{EC} + CH_3OH \longrightarrow \text{DMC} + \text{EG} \quad (33)$$

Souza et al. (2013) evaluated IR's performance from technical, economical and environmental standpoints. Accordingly, the authors proposed a process flowsheet with two serial reactors' system followed by an integrated separation section, with extractive distillation using methyl-iso-butyl ketone (IR-MIBK) and ethylene glycol (IR-EG). For environmental performance assessment, Souza et al. (2013) defined Chemical Sequestration of CO_2 (CSC) as the amount of CO_2 consumed by chemical reaction minus the amount of CO_2 emitted by heat, power and purges. Considering a production of 1.3×10^5 t/y of DMC produced, the authors reported CSC values for IR−MIBK and IR−EG of -15.9kt/y and -8.1kt/y, respectively. The negative values of CSC indicate that both alternatives are net emitters and illustrates that fixation of CO_2 in chemical products does not necessarily imply into net CO_2 reduction, and that the main aspect in CO_2 utilization as feedstock is of substituting fossil carbon source for a renewable alternative. Furthermore, Souza et al. (2013) estimated net present values for IR−MIBK and IR−EG of 71.5×10^6 and 106.5×10^6, respectively, and payback times of 5.5 and 4.5, respectively, concluding for economic feasibility of DMC production. It is worth noting that DMC production from CO_2 is already in use at Asahi Chemical Industry.

4.6. Biochemical conversion of CO_2

Biofixation of CO_2 with microalgae is a promising route of utilization of CO_2, as it exhibits fast growth (e.g., Picardo et al., 2013a) and produces numerous high-added-value bioproducts (Grima et al., 2003). Additionally, they do not contain lignin, a fact that renders microalgae better adapted to biochemical valorization. As advantages of CO_2 bioconversion with relation to energy crops, microalgae grow in variable climates on non-arable land with non-potable water, releasing competition with food crops, and are able to use direct flue gases as their carbon source (Fernández et al., 2012). Alternatively, to inject directly flue gases into microalgae cultures, adequate design and operation of the carbonation culture system unit are also necessary, otherwise almost all of the CO_2 fed to the culture would be released into the atmosphere. In this aspect, photobioreactors are more appropriated arrangements. Furthermore, photobioreactors provide cell requirements such as light, temperature, pH, and mixing (Fernández et al, 2012).

Chisti (2007) concluded that microalgae are the only alternative for the sustainable production of biodiesel. Accordingly, the fact that microalgae biomass is rich in lipids and are, hence, high energy density feedstock for fuels and chemicals is of relevance. Picardo et al (2013a) proposed a screening procedure for microalgae selection to meet production objectives such as SYNGAS for the production of synthetic fuels, since the biomass, or the residual biomass obtained after

extraction of bioproducts, can be gasified to yield SYNGAS. An attractive alternative in this route is to employ CO_2 as oxidation agent (Butterman and Castaldi, 2007). Butterman and Castaldi (2007) report that the injection of CO_2 and H_2O in gasification increases char reactivity that results in more efficient use of the feedstock with less residual to be post-processed.

According to Grima et al. (2003), production of microalgal biomass can be carried out in fully contained photobioreactors or in open ponds and channels. Biomass productivity depends on species, operational conditions and the choice of ponds (~20g/m^2.d) or photobioreactor (~50g/m^2.d) geometry. Open-culture systems are almost always located outdoors and rely on natural light for illumination while closed photobioreactors may be located indoors or outdoors, although outdoor location is more common. Grima et al. (2003) list as biomass harvesting operations centrifugation, filtration or gravity sedimentation, which may be preceded by a flocculation step.

Microalgae contain lipids and fatty acids as membrane components, storage products, metabolites and sources of energy. Microalgae have been found to contain proportionally high levels of lipids (for some species this value can reach 50% oil by weight), with a convenient fatty acids profile and an unsaponifiable fraction allowing a biodiesel production with high oxidation stability (Grima et al., 2013). Lipid accumulation is promoted by stress, notably by nitrogen starvation (Picardo et al., 2013b).
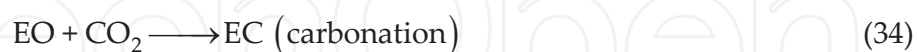
Elemental analysis of carbon content of biomass points to ~50% (Picardo et al., 2013a), what leads to conclude that approximately 2t of CO_2 can be converted into 1t of biomass, potentially amenable to 0.2t of lipids. Its massive extension to the energy sectors constitutes a vast potential for large-volume CO_2 utilization. Fernandez et al. (2012) recognize that microalgae are not a storage strategy because the biomass produced cannot be stored for a long time. Its contribution to reducing CO_2 emissions is only possible if biofuels are produced to replace the fossil fuels use, and allowing the production of other commodities, or by-products from flue gases, which allows one to obtain revenues to mitigate the penalty of carbon capture. To illustrate the potential industrial application of microalgae, Figure 19 shows a schematic of microalgae bioconversion of CO_2 and its downstream processing in a biorefinery arrangement producing long-chain fatty acids (PUFA´s, MUFA´s and PUFA´s), biodiesel, green diesel, gasoline, biogas, urea, N_2 and propylene carbonate.

Monteiro et al. (2010) employed Pareto optimization of what was named an "industrial ecosystem" comprised of a biorefinery of microalgal biomass aiming at maximizing sustainability of the productive arrangement. The authors concluded that increasing the weight of environmental objectives against economic performance might make sectors of the proposed original superstructure of amenable processes unattractive. Therefore, the final structure of a biorefinery of microalgae depends on the priorities set for the productive complex.

4.7. Some pilot and commercial scale CO_2 utilization processes

Polycarbonate: Polycarbonate (PC) is a plastic with impact resistance and heat resistance, mainly produced (4t/y) by reacting CO and Cl_2 to form phosgene as an intermediate material. The phosgene process has a number of disadvantages, including the risk of environmental

Figure 19. Bioconversion of CO_2 integrated into a biorefinery arrangement. Main external inputs are marked in red.

harm (Ushikubo, 2013). Asahi Kasei Corporation succeeded in commercializing the first non-phosgene polycarbonate production using ethylene oxide and CO_2, a by-product of ethylene oxide synthesis. The Asahi Kasei Process has as co-products high-purity monoethylene glycol (MEG). The process employs reactive distillation in the monomer production and gravity-utilized, non-agitation polymerization reactor in the melt polymerization. The monomer process consists of 3 production steps, ethylene carbonate (EC) from CO_2 and EO, dimethyl carbonate (DMC) and MEG from EC and MeOH, and diphenyl carbonate (DPC) and MeOH from DMC and phenol (PhOH). All intermediates are recycled. The by-produced PhOH is recycled to the monomer process (Sinshuke et al., 2010). According to Ushikubo (2013), the new process reduces CO_2 emissions by 0.173kg per one kg of polycarbonate. Five commercial plants using the Asahi Kasei process are operating in Taiwan (150,000 t/y), Korea (2 plants of 65,000 t/y), Russia (65,000 t/y) and Saudi Arabia (260,000 t/y) (Shinsuke et al., 2010).

Monoethylene glycol (MEG): MEG is used as an antifreeze and as a raw material for the production of polyester fibers and resins, mainly PET (Ushikubo, 2013). An expanding market share is foreseen in natural gas industry, where MEG is added into the pipeline or the gas conditioning process, either as hydrate inhibitors or for dehydration purposes to protect downstream pipelines. The pipeline can extend for thousands of kilometers and MEG is injected to inhibit hydrate formation, avoiding plugging (*e.g.,* Statoil´s Snøhvit field, Pettersen, 2011). Concerning the production process, a new technology was developed by Mitsubishi Chemical Corporation with 99% selectivity while the conventional (non-catalytic) process has

selectivity around 89% (Kawabe, 2010). The conventional technology produces as co-product DEG and TEG (di- and triethylene glycols, whose demand is expanding at only 2-3% as opposed to MEG expansion (world demand amounts to 17t/y). Mitsubishi technology uses a two-step catalytic synthesis: production of ethylene carbonate (EC) as intermediate followed by EC hydrolysis under almost stoichiometric condition, while the conventional hydrolysis occurs at a higher H_2O/ethylene oxide molar ratio, according to Eqs. (34) and (35).

$$EO + CO_2 \longrightarrow EC \left(\text{carbonation}\right) \tag{34}$$

$$EO + H_2O \longrightarrow EG + CO_2 \left(\text{hydrolysis}\right) \tag{35}$$

The product purification is simpler (water removal and MEG purification distillation columns, while the conventional process has 4 distillation columns: water, MEG, DEG and TEG columns). Furthermore, CO_2 remains in closed loop. Ushikubo (2013) reports that several commercial plants operating with the new (and greener) technology save resources and energy and reduces the amount of wastewater and CO_2 production. It is worth noting that MEG is a co-product of the production of DMC in a process where Eq. (4.24) is replaced by Eq. (40).

Polyurethane: Bayer (2013) targets the production of polyurethane, via the utilization of CO_2 as feedstock. In this route, CO_2 is converted to polyols (HO-R-OH) which reacts with isocyanate to yield polyurethane. The conversion of CO_2 starts with its reaction with an epoxide, (propylene oxide) of higher energy content, in a catalytic route. Polyol with 30%CO_2 had 2.64 kg of equivalent CO_2 emissions. A maximum theoretical value of 43% of CO_2 can be incorporated in the polyol (Bayer, 2010). The development started in 1669, ended its laboratory scale in 2009, and is moving to industrial implementation of the named "Dream Production" with a pilot plant in Leverkusen to produce polyol, for testing purposes. In early 2013, the new method was successfully converted from the production of discrete quantities to continuous production, a key intermediate step for the industrial-scale production of CO_2-based polyurethane, which Bayer is targeting for 2015.

4.8. Emerging CO_2 utilization processes

The fixation of CO_2 into chemicals and polymers will not substantially contribute to a reduction in antropogenic GHG emissions given the current energy demand. Nevertheless, using CO_2 as a feedstock meets the requirements of sustainable development. An insight into advanced process concepts focus on chemical sequestration of CO_2 creating manufactured products from captured CO_2 with large potential markets. Integration of capture technologies into energy production schemes or oil and gas refining installations is the idea behind cPSE approach, namely, to abate chemical emissions while producing industrial products.

Formic acid: According to Armstrong et al. (2013), the amount of energy required to utilize carbon dioxide as a feedstock largely depends on the oxidation state of the intended products. The next-highest oxidation state molecules from CO_2 are formic acid (HCOOH) and carbon

monoxide (CO). So, carbon dioxide utilization to manufacture formic and other carboxylic acids is a relatively low-energy transformation. Formic acid has numerous applications, including food technology, agriculture, and the leather and rubber industries. Moreover, it has recently been considered as a promising candidate material for hydrogen storage and it is an important chemical with numerous applications. Moreover, formic acid has limited uses for further conversion, except reduction to methanol. The industrial methods used for its production employ CO as a raw material. Maihom et al. (2013) concluded that a first step occurs where CO_2 is hydrogenated to a formate intermediate. In the second step, the formate is further hydrogenated into formic acid. The hydrogenation of CO_2 would complete the chemical loop for hydrogen storage using CO_2. The complementary step is the catalyzed decomposition of formic acid to pure H_2 and reusable CO_2.

Carbon dioxide-based copolymers: The synthesis of organic carbonates has been one of the most widely studied areas of CDU. Typically, CO_2 is inserted into a molecule without the loss of any atoms in either the co-reactant or the gas itself (Armstrong, 2013). Carbonates are formed by the insertion of a CO_2 molecule into a guest co-reactant, typically an epoxide. Poly(propylene carbonate) (PPC), an alternating copolymer of CO_2 and propylene oxide, is one of the emerging low-cost biodegradable plastics. The fast development in catalyst design and performance improvement for PPC has created new chances for the chemical industry. In particular, high molecular weight PPC from rare earth ternary catalyst is becoming an economically viable biodegradable plastic with tens of thousands of tons produced per year, providing a new solution to overcoming the problem of high cost in biodegradable plastics (Qin and Wang, 2010). According to Qin and Wang (2010), with the continuous improvement in catalyst systems, commercialization of CO_2 copolymer is possible. The authors report industrial activities by Empower Materials producing polypropylene carbonate (QPAC®40), polyethylene carbonate (QPAC®25), polybutylene carbonate (QPAC®60), and polycyclohexene oxide(QPAC®130) on a pilot scale.

Electrochemical Reduction of CO_2. Delacourt (2010) studied the electrochemical conversion of CO_2 into SYNGAS. The driver of the proposed route is that renewable energies (e.g., solar and wind) are only alternatives to fossil fuel as they are not available on demand, thus requiring storage. Delacourt (2010) lists as a storage opportunity the conversion to liquid fuels (e.g., methanol), in which SYNGAS is the required intermediate, by converting solar energy into electricity through photovoltaic arrays, and then by using this electricity to produce fuels by electrolysis. Evolved H_2 reacts with CO_2 in a water-gas-shift reactor to make CO (and H_2O). The resulting SYNGAS is converted to methanol. Delacourt (2010) decided for a low-temperature technology (room temperature) although reported that high-temperature electrolysis (800 to 900°C) could be an attractive alternative. Because of the relatively low solubility of CO_2 in water under ambient conditions, gas-diffusion electrodes were applied to operate at higher current densities, and ion-exchange membrane was used as the electrolytic medium to limit gas crossover resulting in a decrease of the current efficiency of the electrochemical cell. Catalysts capable of reduction of CO_2 to CO at low overpotentials were selected.

Light-Driven Technologies. The rubisco enzyme is probably the most abundant enzyme of the biosphere. The fixation of CO_2 and its transfer to organic substrates in the Calvin cycle

leads by way of starch to an annual production of 10^{11} t of biomass (Walther et al., 1999). With the development of catalysts able to reproduce the key steps of photosynthesis, water and sunlight would ultimately be the only needed sources for clean energy production. Light driven technologies under development include (a) photoelectrochemical cells where CO_2 present in a moistened gas stream is converted into organic molecules based on the photooxidation of water into oxygen gas O_2, protons H_+, and electrons. The conversion of CO_2 occurs at the photocathode and involves the generated protons, electrons and the "fuel" CO_2 (Kayaert et al., 2013); (b) direct water oxidation - photocatalytic water splitting - to produce H_2 and O_2 over a metal-oxide-based photocatalyst using solar energy (Maeda and Domen, 2013); (c) hydrogen-producing systems consisting of a hydrogen-evolving catalyst linked to a photosensitizer (Badura et al., 2012). Although promising alternatives, biomimetic CO_2 conversions are still in its early stage of technological development.

CO_2 Mineralization for Environmental Remediation: Lim et al. (2013) reviewed the application of carbonation to solidify or stabilize solid combustion residues from municipal solid wastes, paper mill wastes, etc. and contaminated soils, and to manufacture precipitated calcium carbonate. For instance, the red mud - a highly alkaline waste of Bayer's process - can be treated by absorption of CO_2. Machado (2012) analyzed the process of red mud carbonation with the exhausted gases from the alumina production calcinators, by developing a dynamic model representative of the mass and energy balances involved in the process, and chemical reactions occurring in the mud under carbonation. Machado (2012) was able to predict the species behavior, as well as the decrease in mud pH and the rebound phenomenon observed when the CO_2 concentration is reduced. The transient profile of the main process responses indicated a substantial reduction of CO_2 concentration in the output gas, in consequence of tons of CO_2 captured, and a significant reduction in mud pH. Concerning other environmental applications, Lim et al. (2013) report that carbonated products can be utilized as aggregates in the concrete industry and as alkaline fillers in the paper (or recycled paper) industry. Mineral carbonation consist in reacting CO_2 and Ca or Mg-bound compounds such as wollastonite (CaSiO3), olivine (Mg2SiO4), and serpentine ($Mg_3Si2O_5(OH)_4$). As a result, CO_2 is stably stored in final products such as $CaCO_3$ and $MgCO_3$. Last, the accelerated carbonation of solid wastes containing alkaline minerals such as Ca and Mg before their landfill treatment is effective for decreasing the mobility of heavy metals by adjusting pH to below 9.5 at which their solubility is lowest.

4.9. Non-conversion utilization of CO_2

CO_2 utilization that does not involve its chemical conversion is an alternative destination of captured emissions. Among such alternatives the injection of supercritical CO_2 into depleted oil wells to enhance the further recovery of oil is well established. Indeed, this is presently the only commercially viable technology adding value to large volumes to CO_2 in the order of magnitude of emissions from fossil fuel based energy generation. It has been estimated that CO_2 injection can enhance oil recovery from a depleting well by about 10 to 20 % of the original oil in place. Similarly, CO_2 can be used to recover methane from unmined coal seams. It has been estimated that, in the U.S. alone, 89 billion barrels of oil could technically be recovered using CO_2, leading to a storage of 16 Gt of CO_2 in the depleted oil reservoirs (DNV, 2011).

The use of supercritical CO$_2$ as a solvent in processing chemicals (e.g., flavor extraction) is also well established. New uses of supercritical CO$_2$ in chemical processing are emerging, and have the added benefit of reducing water usage. Supercritical CO$_2$ is also being explored as a heat transfer fluid for some geothermal applications. These non-conversion methods of utilization constitute a significant fraction of the total CO$_2$ emissions (DNV, 2011).

Enhanced Oil Recovery (CO$_2$-EOR): Through CO$_2$-EOR, oil producers inject CO$_2$ into wells to help sustain production in otherwise declining oil fields. The main goal of this technology is to draw more oil to the surface. In 2012, CO$_2$-EOR accounted for 6% of current U.S. domestic oil production. The limited CO$_2$ source is the main barrier to reaching higher levels of CO$_2$-EOR production due to insufficient supplies of affordable CO$_2$. With the discovery of offshore gas fields with high CO$_2$ contents in Brazil, there is a great opportunity to implement CO$_2$-EOR at those fields.

Furthermore, the offshore removal of acid gases poses a choice of onshore processing against offshore processing. Factors like safety and operability may favor onshore processing in comparison with offshore processing. The proper on land disposal of the CO$_2$ removed from natural gas requires the construction of CO$_2$ pipelines to transport CO$_2$ to offshore EOR applications. Another aspect is the high cost of ship hulls as shifting CO$_2$ removal to onshore facilities releases the weight shipped, which could overload the cost of building the required CO$_2$ pipelines.

In the option of onshore processing, CO$_2$ rich natural gas would be available as feedstock to SYNGAS production from CO$_2$ reforming, besides CO$_2$ separation and transport back to oil fields for CO$_2$-EOR. The current estimated cost gap for CGS from power, steel and cement plants is several times larger than the current CO$_2$ market price, and downward pressure on this market price is likely to increase. Investments in CO$_2$ reuse technologies need to be assessed as a screening procedure among potential alternatives.

5. Concluding remarks

Technologies for utilization of CO$_2$ amenable to commercial scales are presently a very small fraction of anthropogenic CO$_2$ emissions, and very endothermic due to the inertness of CO$_2$, what reduces their abatement potential. Furthermore, chemical and biochemical conversion of CO$_2$ presents a sequestration potential that is orders of magnitude lower than the CO$_2$ emissions associated to energy generation from fossil fuels.

Geographical synergies of CO$_2$ supply (power plant emissions or natural gas processing) should guide in the medium term feasible utilization alternatives. The main synergy is identified in offshore gas processing and EOR, which, due to the economic benefit, process scale and maturity, stands as the most relevant utilization route in the short to medium term. Furthermore, most of the emerging alternatives reviewed are at their early stage of techno-logical development.

However, CO$_2$ stands as a promising renewable feedstock to the chemical industry, which has been limited to oil, natural gas, coal and, recently, biomass. Such as posed, SYNGAS based

conversions to the downstream supply chain is a route for flexibility of raw materials. Gasification of a variety of feedstock can lead to SYNGAS. Furthermore, expanding non-conventional gas supply enforces natural gas reforming in the upstream of the chemical supply chain. CO_2 captured from emissions and natural gas processing may drop into the supply chain via Dry Reform. As SYNGAS derived products, hydrogen, methanol and synthetic fuels (e.g., olefins, naphta, diesel, lubricants and kerosene) from Fischer-Tropsch process are likely to dominate the scenario.

Additionally, methanol (MeOH) is expected to grow in relevance either as hydrogen carrier and as intermediate product such as feedstock to MeO (Methanol to Olefins) process, as well as trans-esterification agent in biodiesel and dimethyl carbonate (DMC) production processes. Nowadays, the interest in DMC has grown significantly because it is considered to be a safe and nontoxic substitute for well-established methylating and carbonylating agents (e.g., phosgene), and has potential as an oxygen-containing fuel additive. There are several techno-logical routes to produce DMC, however, the one route considered promising for large-scale commercialization is the trans-esterification of ethylene carbonate (EC) with methanol. In this indirect route, EC is obtained by a previous reaction of CO_2 with ethylene oxide. The route yields DMC and ethylene glycol (EG) as co-products in equimolar ratio.

The use of CO_2 as a carbon source in the synthesis of chemicals, in contrast to disposal, reduces dependence on fossil fuels, generates profit and is in line with a sustainable chemical industry. However, the actual use of CO_2 corresponds to about 0.4% of the potential CO_2 suitable to be converted to chemicals (Navarro et al., 2013).

Finally, large-scale utilization of CO_2 require energy efficient CO_2 capture technologies and an expansion of CO_2 transportation infrastructure.

Acknowledgements

Author details

Ofélia de Queiroz F. Araújo[1], José Luiz de Medeiros[1] and Rita Maria B. Alves[2,3]

1 Federal University of Rio de Janeiro, Brasil

2 BRASKEM S.A., Brasil

3 University of São Paulo, Brasil

References

[1] ADEME (Agence de l'Environnement et de la Maîtrise de l'Energie), Panorama des voies de valorisation du CO$_2$ http://www2.ademe.fr/servlet/getDoc?cid=96&m=3&id= 72052&p1= 30&ref=12441 (2010).

[2] Aouissi, A., Al-Othman, Z.A., Al-Amro, A. Gas-Phase Synthesis of Dimethyl Carbo‐ nate from Methanol and Carbon Dioxide over Co1.5PW12O40 Keggin-Type Hetero‐ polyanion. Int. J. Mol. Sci., 11, 1343-1351 (2010).

[3] Aresta, M. Perspectives in the use of carbon dioxide. Quím. Nova, 22 (2), (1999). http://dx.doi.org/10.1590/S0100-40421999000200019

[4] Aresta, M., Aresta, Michele. Carbon Dioxide as Chemical Feedstock, WILEY-VCH Verlag GmbH & Co., (2010).

[5] Armstrong, Katy, Dawson, George and Styring, Peter. Recent Advances in Catalysis for Carbon Dioxide Utilization. The Catalyst Review, vol. 26, issue 2, 6-13, (2012).

[6] Ashcroft, A.T., Cheetham, A.K., Green, M.L.H., Vernon, P.D.F, Partial oxidation of methane to synthesis gas using carbon dioxide Nature 352, 225 - 226 (18 July 1991).

[7] Badura, A., Guschin, D., Esper, B., Kothe, T., Neugebauer, S., Schuhmann, W., Rögn‐ er, M. Photo-Induced Electron Transfer Between Photosystem 2 via Cross-linked Re‐ dox Hydrogels. Electroanalysis 20(10), 1043–1047 (2012).

[8] Bayer. Use of carbon dioxide for the production of plastics. http://www.materials‐ cience. bayer.com/~/media/Bms/Documents/Publications/CO2-Pro‐ jekte_kurz_EN.ashx. Accessed on 11/27/2013 (2013).

[9] Bayer. A Dream Comes True http://solutions.bayertechnology.com/fileadmin/ user_upload/sat_pages/technologyImpulse/articles/A-Dream-Comes-True.pdf. Ac‐ cessed on 11/27/2013 (2010).

[10] Beck, J., R. Johnson, R., Naya, T., Electrochemical Conversion of Carbon Dioxide to Hydrocarbon Fuels, EME 580, Spring (2010).

[11] Bradford, M. C. J., Vannice, M. A., CO$_2$ Reforming of CH$_4$, Catalysis Reviews, Vol. 41(1), 1-42, (1999).

[12] Bustamante, F., Enick, R. Rothenberger,K., Howard, B., Cugini, A., Ciocco, M. Mor‐ reale, B., Kinetic Study of the Reverse Water Gas Shift Reaction in High-Tempera‐ ture, High Pressure Homogeneous Systems, Fuel Chemistry Division Preprints, 47(2), 663, (2002).

[13] Butterman, H.C., Castaldi, M.J. Influence of CO$_2$ Injection on Biomass Gasification. Ind. Eng. Chem. Res., 46, 8875-8886 (2007).

[14] Byron, S.R.J., Loganthan, M., Shantha, M.S., A Review of the Water Gas Shift Reaction. International Journal of Chemical Reactor Engineering 8, 1–32, (2010).

[15] Chisti, Y. Biodiesel from microalgae. Biotechnol Adv, 25, 294–306 (2007).

[16] Cole, E.B., Bocarsly, A.B., Photochemical, Electrochemical, and photoelectrochemical Reduction of Carbon Dioxide, in "Carbon Dioxide as Chemical Feedstock", M. Aresta, Editor, Wiley-VCH Verlag GmbH & Co.: Weinheim. (2010).

[17] de Medeiros, J.L., Versiani, B., Araújo, O.Q.F. A model for pipeline transportation of supercritical CO_2 for geological storage. The Journal of Pipeline Engineering, 4th Quarter, 253-279 (2008).

[18] de Medeiros, J.L., Nakao, A., Grava, W.M., Nascimento, J.F., Araújo, O.Q.F. Simulation of an Offshore Natural Gas Purification Process for CO_2 Removal with Gas Liquid Contactors Employing Aqueous Solutions of Ethanolamines. Industrial & Engineering Chemistry Research, 52, 7074-7089 (2013a).

[19] de Medeiros, J.L., Barbosa, L.C., Araújo, O.Q.F. An Equilibrium Approach for CO_2 and H_2S Absorption with Aqueous Solutions of Alkanolamines: Theory and Parameter Estimation. Industrial & Engineering Chemistry Research, 52, 9203-9226 (2013b).

[20] Delacourt, C. Electrochemical reduction of carbon dioxide and water to syngas (CO + H_2) at room temperature. Available at http://charles.delacourt.free.fr/Postdoc-manuscript_Charles-Delacourt.pdf (2010).

[21] DNV. Carbon Dioxide Utilization Electrochemical Conversion of CO_2 – Opportunities and Challenges. Available online at http://www.dnv.com/binaries/DNV-position_paper_CO2_Utilization_tcm4-445820.pdf (2011).

[22] Edwards, J.H., Potential sources of CO_2 and the options for its large-scale utilisation now and in the future. Catalysis Today, 23, 59-66, (1995).

[23] Ferreira, H.B.P., Vale, D.L., Mota, C.J.A., Miranda, J.L. Experimental Design for CO_2 Conversion into Dimethylcarbonate (DMC) using Bu_2SnO at Subcritical Conditions. Brazilian Journal of Petroleum and Gas, 6(3), 93-104, (2012).

[24] Fernández, F.G.A., González-López, C.V., Sevilla, J.M.F., Grima, E.M. Conversion of CO_2 into Biomass by Microalgae: How Realistic a Contribution May it be to Significant CO_2 Removal? Appl Microbiol Biotechnol, 96, 577–586 (2012).

[25] Gangadharan, P., et al., Evaluation of the economic and environmental impact of combining dry reforming with steam reforming of methane. Chem. Eng. Res. Des. (2012), http://dx.doi.org/10.1016/j.cherd.2012.04.008

[26] Genesis. Equation of State Prediction of Carbon Dioxide Properties. Project Kingsnorth Carbon Capture & Storage Project. CP-GNS-FAS-DRP-0001. http://www.decc.gov.uk/assets/decc/11/ccs/chapter6/6.23-equation-of-state-prediction-of-carbon-dioxide-properties.pdf, (2011).

[27] Ginsburg, J. M.; Pina, J.; El Solh, T.; de Lasa, H. I.Coke formation over a nickel cata‐ lyst under methane dry reforming conditions: Thermodynamic and kinetic models Ind. Eng. Chem. Res., 44 (14) 4846– 4854, (2005).

[28] Grima, E.M., Belarbia, E.-H., Acién Fernández, F.G., Medina, A.R., Chisti, Y. Recov‐ ery of microalgal Biomass and Metabolites: Process Options and Economics. Biotech‐ nology Advances, 20, 491–515 (2003).

[29] Gunardson, H. Industrial Gases in Petrochemical Processing; Marcel Dekker: New York, (1998).

[30] Hartley, M., Tam, I., Non-Sequestration Utilization Options for Carbon Dioxide (CO$_2$), Nexant´s ChemSystems PERP09/10S10, (2012).

[31] Ho, M.T., Wiley, D. E. Economic Evaluation of Membrane Systems for Large Scale Capture and Storage of CO$_2$ Mixtures. Report, UNESCO Centre for Membrane Sci‐ ence, The University of New South Wales (2005).

[32] Hu, B., Guild, C., Suib, S.L., Thermal, electrochemical, and photochemical conversion of CO$_2$ to fuels and value-added products, Journal of CO$_2$ Utilization, 1, 18–27, (2013).

[33] IEA. Technology Roadmap - Energy and GHG Reductions in the Chemical Industry via Catalytic Processes. Technology Perspectives. Available online at: http://iea.org/ media/freepublications/technologyroadmaps/TechnologyRoadmapCatalyticProces‐ sesAnnexes.pdf, (2013).

[34] Jarungthammachote, S., Combined Partial Oxidation and Carbon Dioxide Reforming Process: A Thermodynamic Study, American Journal of Applied Sciences 8 (1): 9-14, (2011).

[35] Jiang, Z.; Liao, X.; Zhao, Y., Comparative study of the dry reforming of methane on fluidized aerogel and xerogel Ni/Al2O3 catalysts. Applied Petrochemical Research, p. 1-9, (2013).

[36] Kahle, L. C. S., Roussière, T., Maier, L., Delgado, K.H., Wasserschaff, G., Schunk, S.A., Deutschmann, O., Methane Dry Reforming at High Temperature and Elevated Pressure: Impact of Gas-Phase Reactions, Industrial & Engineering Chemistry Re‐ search, 52 (34), (2013).

[37] Kaiser, P., Unde, R.B., Kern, C., Jess, A. Production of Liquid Hydrocarbons with CO$_2$ as Carbon Source based on Reverse Water-Gas Shift and Fischer-Tropsch Synthesis. Chemie Ingenieur Technik. Special Issue: Reaktionstechnik. 85(4), 489–499, (2013).

[38] Kawabe, K. Development of Highly Selective Process for Mono-Ethylene Glycol Pro‐ duction from Ethylene Oxide via Ethylene Carbonate Using Phosphonium Salt Cata‐ lyst. Catal Surv Asia 14, 111–115, (2010).

[39] Kayaert, S., Martens, J., Masschaele, K. Photo-Electrochemical Cell. United States Pat‐ ent Application 20130026029, (2013).

[40]   King, D. The Future of Industrial Biorefineries. World Economic Forum, (2010).

[41]   Kuwabata, S., Nishida, K., Tsuda, R., Inoue, H., Yoneyama, H., Photochemical Reduction of Carbon Dioxide to Methanol Using ZnS Microcrystallite as a Photocatalyst in the Presence of Methanol Dehydrogenase, J. Electrochem. Soc. 141(6), 1498, (1994).

[42]   Kuwabata, S., Tsuda, R., Yoneyama, H., Electrochemical Conversion of Carbon Dioxide to Methanol with the Assistance of Formate Dehydrogenase and Methanol Dehydrogenase as Biocatalysts. J. Am. Chem. SoC., 116, 5431-5443, (1994).

[43]   Kurz, G. , Teuner, S., Calcor process for carbon monoxide production, Erdoel & Kohle, Erdgas, Petrochemie, 43(5), 171-172, (1990).

[44]   Lachowska, M., Skrzypek, J., Ga, Mn, and Mg Promoted Copper/Zinc/Zirconia-Catalysts for Hydrogenation of Carbon Dioxide to Methanol, Carbon Dioxide Utilization for Global Sustainability, Elsevier, Amsterdam, (2004).

[45]   Le, M.T.H., Electrochemical Reduction of CO_2 to Methanol, MSc Thesis. Graduate Faculty of the Louisiana State University and Agricultural and Mechanical College, (2011).

[46]   Lee, D., Lee, J.-Y., Lee, J.S., Effects of Palladium Particle Size in Hydrogenation of Carbon Dioxide to Methanol over Pd/ZnO Catalysts, Carbon Dioxide Utilization for Global Sustainability, Elsevier, Amsterdam, (2004).

[47]   Levitan, R., Levy, M., Rosin, H., Rubin, R., Closed-loop operation of a solar chemical heat pipe at the Weizmann Institute solar furnace. Solar Energy Materials vol. 24 issue 1-4, 464-477, (1991).

[48]   Levy, M., Levitan, R., Rosin, H., Rubin, R., Solar energy storage via a closed-loop chemical heat pipe. Solar Energy, vol. 50, issue 2, 179-189, (1993).

[49]   Li, H.. Thermodynamic Properties of CO_2 Mixtures and Their Applications in Advanced Power Cycles with CO_2 Capture Processes. Energy Processes Department of Chemical Engineering and Technology Royal Institute of Technology, Stockholm, Sweden. TRITA-CHE Report 2008:58, (2008).

[50]   Li, H., Yan, J.. Evaluating Cubic Equations of State for Calculation of Vapor–Liquid Equilibrium of CO_2 and CO_2-Mixtures for CO_2 Capture and Storage Processes. Chem. Eng. and Technology/Energy Process, Royal Institute of Technology, (2009).

[51]   Lim, M., Han, G.C., Ahn, J.W., You, K.S. Environmental Remediation and Conversion of Carbon Dioxide (CO_2) into Useful Green Products by Accelerated Carbonation Technology. Int. J. Environ. Res. Public Health, 7, 203-228, (2010).

[52]   Li, M.W., Xu, G.H., Tian, Y.L., Chen, L., Fu, H.F. Carbon dioxide reforming of methane using DC corona discharge plasma reaction. J. Physical Chem. A., 108: 1687-1693, (2004).

[53]   Machado, R.B.P. Avaliação Técnica de Processo de Carbonatação de Lama Vermelha com Gás Exausto de Calcinadores de Alumina. MSc Thesis. Graduate Program in

Chemical and Biochemical Process Technology, School of Chemistry, Federal University of Rio de Janeiro, (2012).

[54] Maeda, K. Domen, K. 7.22 – Photochemical Water Splitting Using Nanostructured Metal Oxides. Reference Module in Chemistry, Molecular Sciences and Chemical Engineering Comprehensive Inorganic Chemistry II (Second Edition). From Elements to Applications, 587–614. Vol. 7: Surface Inorganic Chemistry and Heterogeneous Catalysis, (2013).

[55] Maiohm, T., Wannakao, S., Boekfa, B., Limtrakul, J. Production of Formic Acid via Hydrogenation of CO$_2$ over a Copper-Alkoxide-Functionalized MOF: A Mechanistic StudyJ. Phys. Chem. C, 117, 17650–17658, (2013).

[56] McCoy, S.T. The economics of CO$_2$ transport by pipeline and storage in saline aquifers and oil reservoirs. PhD Thesis, Carnegie-Mellon University, Pittsburgh, USA, (2008).

[57] Meunier, F.C., Tibiletti, D., Goguet, A., Shekhtman, S., Hardacre, C., Burch, R., On the complexity of the water-gas shift reaction mechanism over a Pt/CeO$_2$ catalyst: Effect of the temperature on the reactivity of formate surface species studied by operando DRIFT during isotopic transient at chemical steady-state, Catalys Today, 126, 143, (2007).

[58] Moon, D.J., Ryu, J.W., Kang, D.M., Lee, B.J., Ahn, B.S., CO$_2$ Reforming by CH$_4$ over Ni-YSZ Modified Catalysts in Carbon Dioxide Utilization for Global Sustainability, Elsevier, Amsterdam, (2004).

[59] Monteiro, J.G.M.S., Silva, P.A., Araújo, O.Q.F., de Medeiros, J.L. Pareto Optimization of an Industrial Ecosystem: sustainability maximization. Brazilian Journal of Chemical Engineering, 27, 429-440, (2010).

[60] Nakao, A., Macedo, A.P.F., Versiani, B.M., Araújo, O.Q.F., and de Medeiros, J.L., Modeling of Flowcharts of Permeation through Membranes for Removal of CO$_2$ of Natural Gas, 10th International Symposium of Process System Engineering, PSE-2009, Computer Aided Chemical Engineering, 27, 1875-1880, ISBN 978-0-444-53472-9, Elsevier, (2009)

[61] Navarro, R., Pawelec, B., Alvarez-Galván, M. C., Guil-Lopez, R. Al-Sayari, S., Fierro, J. L. G. Renewable SYNGAS Production via Dry Reforming of Methane, in M. de Falco et al., CO2: A Valuable Source of Carbon Green Energy and Technology, pp 45-66, Spring-Verlag London, (2013).

[62] Nagaoka, K., Seshan, K., Aika, K., Lercher, J.A., Carbon deposition during carbon dioxide reforming of methane-comparison between Pt/Al$_2$O$_3$ and Pt/ZrO$_2$. J. Catalysis, 197: 34-42, (2001).

[63] O'Connor A.M., Ross J.R.H. The Effect of O$_2$ Addition on the Carbon Dioxide Reforming of Methane over Pt/ZrO$_2$. Catalysts. Catal. Today, 46 (2-3), 203–210, (1998).

[64] Oi, L.E. CO$_2$ removal by absorption: challenges in modelling. Mathematical and Computer Modelling of Dynamical Systems, 16(6), 511–533 (2010).

[65] Olah, G.A., Goeppert, A., Prakash, G.K.S., Beyond Oil and Gas: The Methanol Economy, 2nd ed., Wiley VCH, Weinheim, Germany, (2009).

[66] Olah, G.A., Goeppert, A., Prakash, Czaun, M., G.K.S., Bi-reforming of Methane from Any Source with Steam and Carbon Dioxide Exclusively to Metgas (CO–2H$_2$) for Methanol and Hydrocarbon Synthesis, J. Am. Chem. Soc., 135 (2), 648–650, (2013).

[67] Ormerod, W., Riemer, P., Smith, A. Carbon Dioxide Utilisation. IEA Greenhouse Gas R&D Programme, http://www.ieagreen.org.uk/sr4p.htm, (1995).

[68] Pettersen, J. Snøhvit field development. Available online at http://www.ipt.ntnu.no/~jsg/ undervisning/prosessering/gjester/LysarkPettersen2011.pdf, (2011).

[69] Petrobras. Visão Geral da Petrobras. Available online at: http://www.investidorpetrobras.com.br/pt/apresentacoes/visao-geral-da-petrobras.htm

[70] Pettersen, J., Snøhvit field development, TEP4520, Statoil, (2011).

[71] Picardo, M.C., de Medeiros, J.L., Monteiro, J.G.M., Chaloub, R.M., Giordano, M., Ofélia, Q.F. A methodology for screening of microalgae as a decision making tool for energy and green chemical process applications. Clean Technologies and Environmental Policy, 15, 275-291, (2013a).

[72] Picardo, M.C., de Medeiros, J.L., Ofélia, Q.F., Chaloub, R.M. Effects of CO$_2$ Enrichment and Nutrients Supply Intermittency on Batch Cultures of Isochrysis galbana. Bioresource Technology, 143, 242-250, (2013b).

[73] Qin, Y., Wang, X. Carbon dioxide-based copolymers: Environmental benefits of PPC, an industrially viable catalyst. Biotechnol. J., 5, 1164–1180, (2010).

[74] Raju, A.S.K., Park, C.S., Norbeck, J.M., Synthesis gas production using steam hydrogasification and steam reforming. Fuel Process. Technol. 90, 330–336, (2009).

[75] Richardson, J.T., Paripatyadar, S.A. , Carbon dioxide reforming of methane with supported rhodium Appl. Catal. 61, 293-309, (1990).

[76] Rostrup-Nielsen, J., 40 years in catalysis, Catalysis Today, 111, 4-11, (2006).

[77] Rostrup-Nielsen, J., Christiansen, L.J. Concepts in syngas Manufacture. Catalytic Series, V. 10. World Scientific, 392 pp, 2011. ISBN: 978-1-84816-567-0, (2011).

[78] Saito, M., Murata, K., Development of high performance Cu/ZnO-based catalysts for methanol synthesis and the water-gas shift reaction, Catalysis Surveys from Asia, 8, 285-294, (2004).

[79] Sakakura, T., Choi, J., Yasuda, H. Transformation of carbon dioxide. Chem Rev, 107, 2365-2387, (2007).

[80] Shinsuke, F., Isaburo, F., Masahiro, T., Kazuhiro, O., Hiroshi, H., Muneaki, A., Kazumi, H., Kyosuke, K. A Novel Non-Phosgene Process for Polycarbonate Production from CO$_2$: Green and Sustainable Chemistry in Practice. Catalysis surveys from Asia, 14(3-4), 146-163, (2010).

[81] Song, C., Pan, W., Tri-Reforming of Methane: A Novel Concept for Synthesis of Industrially Useful Synthesis Gas with Desired H$_2$/CO Ratios Using CO$_2$ in Flue Gas of Power Plants without CO$_2$ Separation, Prepr. Pap.-Am. Chem. Soc., Div. Fuel Chem., 49 (1), 128, (2004).

[82] Song, C. Global Challenges and Strategies for Control, Conversion and Utilization of CO$_2$ for Sustainable Development Involving Energy, Catalysis, Adsorption and Chemical Processing. Catalysis Today, 115, 2–32, (2006).

[83] Souza, M.M.V.M., Schmal, M., Methane conversion to synthesis gas by partial oxidation and CO$_2$ reforming over supported platinum catalysts, Catalysis Letters, 91(1–2), 11-17, (2003).

[84] Souza, L.F.S., Ferreira, P.R.R., de Medeiros, J.L.M., Alves, R.M.B., Araŭjo, O.Q.F. Production of DMC from CO$_2$ via Indirect Route: Technical−Economical−Environmental Assessment and Analysis Sustainable Chem. Eng., dx.doi.org/10.1021/sc400279n, (2013).

[85] Span, R., Wagner, W. A New Equation of State for Carbon Dioxide Covering the Fluid Region from the Triple-Point Temperature to 1100 K at Pressures up to 800 MPa. J. Phys. Chem. Ref. Data, 25(6), (1996).

[86] Spath, P.L., Dayton, D.C., Preliminary Screening – Technical and Economic Assessment of Synthesis Gas to Fuels and Chemicals with Emphasis on the Potential for Biomass-Derived SYNGAS. National Renewable Energy Lab Golden Co., (2003).

[87] Stoczynski, J., Grabowski, R., Koslowska, A., Lachowska, M., Skrzypek, J., Effect of Additives and a Preparation Method on Catalytic Activity of Cu/ZnO/ZrO$_2$ System in the Carbon Dioxide Hydrogenation to Methanol, Carbon Dioxide Utilization for Global Sustainability, Elsevier, Amsterdam, (2004).

[88] Tanaka, Y., Utaka, T., Kikuchi, R., Sasaki, K., Eguchi, K., CO removal from reformed fuel over Cu/ZnO/Al2O3 catalysts prepared by impregnation and coprecipitation methods, Applied Catalysis A: General, 238, 11–18, (2003).

[89] Teuner, S., Make carbon monoxide from carbon dioxide, Hydrocarbon Processing, International Edition, 64(5), 106-7, (1985).

[90] Teuner, S. et al., The Calcor Standard and Calcor Economy Processes, in Oil and Gas European Magazine, 44-46, (2001).

[91] Treacy, D., Ross, J.R.H. The Potential of the CO$_2$ reforming of CH$_4$ as a method of CO$_2$ mitigation. A thermodynamic study. Prepr. Pap.-Am. Chem. Soc., Div. Fuel Chem., 49 (1), 126–127, (2004).

[92] Trusler, J. P. M. Equation of State for Solid Phase I of Carbon Dioxide Valid for Temperatures up to 800 K and Pressures up to 12 GPa. J. Phys. Chem. Ref. Data, 40 (4), 043105-1-043105-19, http://dx.doi.org/10.1063/1.3664915, (2011).

[93] Van-Dal, E.S., Boualloub, C. Design and simulation of a methanol production plant from CO_2 hydrogenation. Journal of Cleaner Production, 57, 15 October 2013, 38–45, http://dx.doi.org/10.1016/j.jclepro.2013.06.008

[94] Ushikubo, T. Green Chemistry in Japan. Chemistry International, 35(4), July-August 2013. Available online at www.iupac.org/publications/ci, (2013).

[95] Wagener, D.H.V., Rochelle, G.T. Alternative Stripper Configurations for CO_2 Capture by Aqueous Amines. AIChE Spring Meeting, (2010).

[96] Wagener, D.H.V., Rochelle, G.T. Stripper configurations for CO_2 capture by aqueous monoethanolamine. Chemical Engineering Research and Design, 89, 1639–1646, (2011).

[97] Walther, D., Ruben, M., Rau, S. Carbon Dioxide and Metal Centres: from Reactions Inspired by Nature to Reactions in Compressed Carbon Dioxide as Solvent. Coordination Chemistry Reviews 182, 67–100, (1999).

[98] Wang, W., Stagg-Williams, S.M., Noronha, F.B., Mattos, L.V.,Passos, F.B., Partial Oxidation and Combined Reforming of Methane on Ce-promoted Catalysts, Prepr. Pap.-Am. Chem. Soc., Div. Fuel Chem. 49 (1), 132-133, (2004).

[99] Wu, J.C.S., Lin, H.-M., Photo reduction of CO_2 to methanol via TiO_2 Photocatalyst, International Journal of Photoenergy, 7, 115-119, (2005).

[100] Wurzel, T., Malcus, S., Mleczko, L., Reaction engineering investigations of CO_2 reforming in a fluidized-bed reactor. Chem. Eng. Sci., 55, 3955-3966 (2000).

[101] Yamashita, H., Fujii, Y., Ichihashi, Y., Zhang, S. G., Ikeue, K., Park, D. R.,Koyano, K., Tatsumi, T., Anpo, M., Selective formation of CH_3OH in the photocatalytic reduction of CO_2 with H_2O on titanium oxides highly dispersed within zeolites and mesoporous molecular sieves, Catalysis Today 45, 221-227, (1998).

[102] Zangouei, M., Moghaddam, A.Z., Razeghi, A., Omidkhah, M.R., Reforming and Partial Oxidation of CH_4 over Ni/Al_2O_3 Catalysts in Fixed-bed Reactor International Journal of Chemical Reactor Engineering, 8. Available at: http://works.bepress.com/mohammadreza_omidkhah/2, (2010).

[103] Zhang, X., Lee, C. S.-M., Mingos, D.M.P., Hayward, D. O., Carbon dioxide reforming of methane with Pt catalysts using microwave dielectric heating. Catalysis Letters, 88(3–4), 129-139, (2003).

[104] Zhou, H., Cao, Y., Zhao, H., Liu, H., Wei-Ping, P., Investigation of H_2O and CO_2 Reforming and Partial Oxidation of Methane : Catalytic Effects of Coal Char and Coal Ash, Energy & Fuels, 22, 2341-2345, (2008).